MASSACHUSETTS INSTITUTE OF TECHNOLOGY
AEROPHYSICS LABORATORY

Technical Report 89

A STUDY OF ATMOSPHERIC EFFECTS ON SONIC BOOMS

by

Manfred P. Friedman

April 1964

Massachusetts Institute of Technology
Department of Aeronautics and Astronautics
Aerospace Research Division
Aerophysics Laboratory

Technical Report 89

A STUDY OF ATMOSPHERIC EFFECTS ON SONIC BOOMS

by

Manfred P. Friedman

Contract NAS 1-2511
DSR 9398

April 1964

FOREWORD

The work done on this project was supported by NASA, Contract NAS 1-2511. Some of the computer work was done at the Computation Center at MIT, Cambridge, Massachusetts.

The author wishes to thank Mr. Charles Bartlett of MIT for his many helpful suggestions.

ABSTRACT

3289/

An approach to the problem of a shock propagating through a variable atmosphere is presented. A previously presented theory has been improved and a computer program has been written using the results of the improved theory. This paper presents the improved results and gives a detailed description of the computer program.

For an atmosphere which varies arbitrarily in the vertical direction and for a supersonic aircraft with arbitrary lift and volume distribution the computer program will give the shock overpressure and intersection points at the ground. In addition, effects due to aircraft acceleration, flight path angle and curvature and acoustical cutoff are computed and presented by the program.

Author

TABLE OF CONTENTS

SECTION I

INTRODUCTION

This report will give a description of a "Sonic Boom Computer Program".* The theoretical development, upon which the computer program is based, is presented in Section IV and Appendix 1. Since the emphasis here is for the operation of the SBCP, discussion of the theoretical results will be kept to a minimum.

The SBCP uses the following input data:

1) Atmospheric pressure, temperature and winds between the aircraft and the ground, and shock-ground reflection factor.

2) Aircraft parameters such as Mach number, altitude, acceleration rate, volume and lift factors, aircraft length and weight.

3) The analysis is based on ray tube concepts, that is, a small segment of shock is considered to be propagating down a ray tube and its strength and location are determined along the ray path until it strikes the ground. Therefore, another input is the initial ray directions. These are specified by giving those angles, measured around the flight direction, for which computations are desired. (That is, the angles Φ in Fig. 1, Section II).

The computer output gives:

1) A listing of pertinent input data.

2) The location and strength of the shock corresponding to a selected input angle at intermediate computed points between the aircraft and the ground.

3) The location and strength of the shock at the shock-ground intersection.

The program was written in Fortran and has been operated on IBM 709, 7090 and 7094 computers.

---

* In the remainder of this report the "Sonic Boom Computer Program" will be denoted by SBCP.

Details for operating the program are given in Section II. The equations which are actually solved are presented in Section III. In addition the Fortran symbols and their corresponding physical variables and a brief descriptions of the subroutines are given in this section. Some improvements to the theory are given in Section IV. The paper in which the general theory was presented is reproduced in Appendix 1. In Appendix 2 the input and output for two sample problems are given. A listing of the Fortran instruction cards is given in Appendix 3.

In Appendix IV the theory is extended to include aircraft diving or climbing and curved flight path effects. Since the original version of this report (TR 89, Dec. 1963) appeared, these aircraft maneuver calculations have been included in the SBCP. The present report includes everything that was in TR 89 plus the above improvements.

Results of some sample computations are given in Appendix V.

SECTION II

PROGRAM OPERATION DETAILS

II.1 INPUT FORMAT

In order to operate the program the data cards must be arranged in the following manner:

Control card: The first card is a control card, it tells the following:

1) The number of altitudes at which atmospheric data will be prescribed, this number can be 2 to 100. That is a minimum of 2 altitudes (aircraft and ground) are required to run any problem and a maximum of 100 altitudes can be handled. This number should be entered so that the last digit is in column 10.

2) The number of angles, measured about the aircraft axis, for which output data is desired (see "angle cards", p.4). A minimum of 1 and a maximum of 21 different angles can be prescribed, therefore this number can be 1 to 21. It should be entered so that the last digit is in column 20.

3) A problem identification number. This can be any integer from 0 to 99999. It should be entered so that the last digit is in column 30.

4) The input angles mentioned in (2) above can be entered in any order. However it is necessary to know which of these angles corresponds to the direction directly below the aircraft. The next entry on the control card tells which of the input angles corresponds to this direction. This can therefore be a number between 1 and 21. It should be entered so that the last digit is in column 40.

5) Part of the output is a listing of the shock strength and location for one of the input angles at computed points between the aircraft and the ground. That is, a time history of the shock propagation is given. The next entry tells which one of the input angles this information should correspond to. This can therefore be a number between 1 and 21. It should be entered so that the last digit is in column 50.

6) The last entry on the control card tells the computer whether or not another problem (different atmosphere, different aircraft, etc.) follows the completion of the problem currently being entered. A negative number in columns 51 to 60 will stop the computer at the end of the current computation; no entry or a positive entry will have the computer read in a new set of data after completion of the current problem.

All the numbers entered on the control card are fixed point integers. That is, no decimal point should be used and the first five entries should appear in the columns indicated. The last entry (if any) can go anywhere between columns 51 and 60.

Atmosphere Cards: After the control card the next cards carry atmospheric data. There will be one card for each altitude at which atmospheric data is prescribed. (The number of atmosphere cards is equal to the first number entered on the control card.)

These cards are entered so that the highest altitude is first, then descending in altitude, and the lowest altitude (ground) last. Each card has the same format and tells the altitude and the pressure, temperature, headwind and sidewind corresponding to that altitude. All numbers must have their decimal point and can appear anywhere within the columns indicated below.

Columns	Data	
1 – 10	altitude ÷ 1000.	in feet
11 – 20	pressure	pounds/sq.ft.
21 – 30	temperature	deg. F
31 – 40	headwind	ft./sec.
41 – 50	sidewind	ft./sec.

The winds should be referenced to the aircraft direction. A headwind is positive and a tailwind is negative. A sidewind in the direction of the starboard wing is positive, in the direction of the port wing is negative.

Angle cards: The computation starts with an initial ray direction and determines shock properties all along this ray until it meets the ground. The initial ray directions are determined by the "angle input", these are angles measured about the aircraft ray (or shock) cone axis. The angle $\phi = 0$

corresponds to directly below the aircraft. In Fig II.1 the aircraft is moving in the direction of the negative x axis and is coming out of the paper toward the reader.

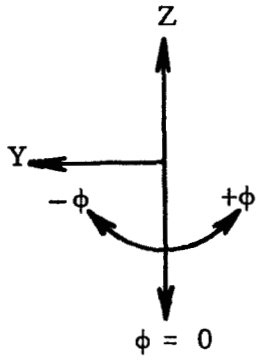

$\phi = 0$ corresponds to directly below the aircraft

Figure II. 1

As many as 21 different angles ϕ can be specified, they can be entered in any order and are measured in degrees. The numbers must have their decimal point and are entered 7 numbers per card as follows:

Columns	Data
1 – 10	first angle in degrees
11 – 20	second " " " (if necessary)
61 – 70	seventh " " " "
1 – 10 next card	eighth " " " " , etc.

The angle (with decimal point) can appear anywhere within the indicated columns. The number of successive columns of ten needed for entering all the angles is equal to the second number entered on the control card.

One of the angles entered must be zero ($\phi = 0.0$). The number corresponding to the position of the angle $\phi = 0.0$ in the above array is the fourth entry on the control card. One of the angles can be selected to have a history of the shock properties between the aircraft and the ground printed out, the number corresponding to the position of this angle in the above array is the fifth entry on the control card.

Aircraft data cards: The last input cards give thirteen pieces of data by which the aircraft, flight conditions, and shock-ground reflection factor are specified. For each of these numbers there are ten columns on the input card, the numbers must be entered with their decimal point and can appear anywhere within the field of ten columns. The order of entry is as follows:

Columns	Data
1–10 first card	aircraft acceleration, ft/sec.^{2}
11–20 " "	aircraft length, ft.
21–30 " "	shock-ground reflection constant
31–40 " "	aircraft Mach number
41–50 " "	aircraft altitude, ft.
51–60 " "	aircraft volume factor
61–70 " "	aircraft lift factor
1–10 second card	aircraft weight, lb.
11–20 " "	aircraft fineness ratio (length/max. diameter)
21–30 " "	effective wing length for lift distribution, ft.
31–40 " "	flight path curvature x 10^6 , 1/ft.
41–50 " "	climb (or dive) angle, deg.
51–60 " "	time increment, sec.

The last three entries above involve aircraft dive and climb calculations, they are defined in Appendix IV. Details of the integration of body shape and lift distribution source terms are not carried out in the SBCP. An asymptotic "aircraft shape term" is used (See Section III.1, Eq. III.13). This term is given below:

Shock overpressure at the ground

$$\Delta P = P_g \times RC \times \left\{\begin{matrix}\text{atmospheric and} \\ \text{propagation terms}\end{matrix}\right\} \times \left\{\begin{matrix}\text{aircraft} \\ \text{shape terms}\end{matrix}\right\} \times \left\{\frac{4M^3}{M^2-1}\right\}^{1/4}$$

$$\begin{matrix}\text{aircraft} \\ \text{shape terms}\end{matrix} = \sqrt{\left(\frac{VF \cdot L^{.75}}{FR}\right)^2 + \cos\phi \cdot \frac{\sqrt{M^2-1} \cdot LF^2 \cdot WT}{M^2 \cdot P_h \cdot (WC)^{.5}}}$$

P_g = atmospheric ground pressure

P_h = pressure at aircraft altitude

R_c = reflection constant

M = Mach No.

VF = volume factor

LF = lift factor

WT = aircraft weight

L = " length

FR = " fineness ratio

WC = wing chord for lift distribution

II.2 OUTPUT FORMAT

The output format will be self explanatory, however to itemize:

First: problem number and aircraft data are given

Second: input atmosphere is reproduced

Third: history of shock strength variation for selected input angle is presented

Fourth: shock-ground intersection data are listed

Other possible output information is as follows:

1) If the shock is cutoff by atmospheric refraction, the location and the identification of the corresponding input angle are printed out. Also, whenever posssible, the shock overpressure at cutoff is presented.

2) If aircraft acceleration effects (that is possible high shock overpressures) take place before the shock has propagated 100 body lengths this fact is printed out.

3) If for some reason the computation to determine the pressure jump across the shock does not converge this fact is printed out.

II.3 PROGRAM LIMITATIONS

1) The aircraft altitude must be greater than ground altitude, and less than or equal to the highest altitude for which atmospheric data is prescribed.

2) The shock strength is not computed until it has propagated approximately 100 body lengths from the aircraft. If data is desired closer to the aircraft the computer can be "fooled" by feeding in a small value for body length, L, and increasing the volume factor, VF, so that their product in Eq. (II.1) remains constant. Care should be taken when interpreting the resulting data since the present theory is essentially a far field theory. That is, the far field result would be correct but the results near the aircraft might be questionable.

3) The computation time is essentially proportional to the number of altitude steps taken to carry out the integrations times the number of input angles. The magnitude of the integration step size is one quarter of the smallest altitude spacing. For an aircraft at 60,000 ft. and altitude

data spacing 1000 ft. (step size 250 ft.) there will be about 240 integration steps; computation times on IBM 709, 7090 and 7094 are approximately 10, 2 and 1.5 seconds respectively for each input angle.

SECTION III
PROGRAM DETAILS

III.1 EQUATIONS

The basic theory is given in Appendix I and Section IV, however the equations actually evaluated on the computer are presented in this section. Although the equations were taken directly from the theoretical development they had to be modified slightly for evaluation on a digital computer.

All computations start at the aircraft altitude and work downward along a ray to the ground. The coordinate system used has its origin at the ground directly below the aircraft, hence the computations start at $z = h$ and end at $z = z_{ground}$.

Shock Location:

Equations for the shock location, Eq. (3.10) of Appendix I are integrated directly

$$\left\{ \begin{array}{l} x = \displaystyle\int_h^z \left[\frac{\ell V_s + u_0}{n V_s} \right] dz \\ \\ y = \displaystyle\int_h^z \left[\frac{v_0}{n V_s} \right] dz \\ \\ t = \displaystyle\int_h^z \left[\frac{1}{n V_s} \right] dz \end{array} \right\} \qquad \text{(III.1)}$$

After the ray-ground intersection, as determined from above equations, is computed the coordinates are referred to a fixed coordinate system by the procedure described under the heading "shock-ground intersection" later in this section.

Ray Tube Area

Since we are integrating from altitude z = h downward Eq. (IV.12) becomes, after setting $V_s dt = ds$

$$A = (h - z)\sec \nu_h \left\{ 1 - \frac{\dot{V}_a\, s}{a_h^2\, M(M^2 - 1)} + \frac{\sec \nu_h}{V_a \cos \theta} \int_h^z \tan \nu \left[\frac{dV_s}{dz} - \sin \nu \frac{du_0}{dz} \right] dz \right\} \tag{III.2}$$

where

$$s = \int_h^z \left(\frac{ds}{dz} \right) dz \tag{III.3}$$

and (ds/dz) is given in Eq. (3.10) of Appendix I.

Pressure Jump

There are two integrals involved in the pressure jump expression, Eq. (IV.3). The first, I(s), which is defined before Eq. (2.10) of Appendix I, can be written

$$I(z) = \exp \left\{ \int_{z=h}^{z} \frac{\rho_0\, dw_0 - \left[(\gamma - 1)/2 \right] w_0\, d\rho_0}{\rho_0\, (w_0 + a_0)} \right\} \tag{III.4}$$

This is simply an integration of atmospheric variables between aircraft altitude and altitude z. Therefore the quantity, I, can be considered as another atmospheric variable which can be derived from input data.

In order to evaluate Eq. (III.4), the density, ρ_0, was expressed in terms of pressure and sound speed

$$\frac{d\rho}{\rho} = \frac{dp}{p} - \frac{da}{a} \quad .$$

The second integral in the pressure jump expression

$$\int_0^s \frac{ds}{B}$$

is evaluated in the form

$$J = \int_h^z \frac{ds}{dz} \frac{dz}{B} \quad . \tag{III.5}$$

The quantity B, defined in Appendix 1, is

$$B = (a_0 + w_0)^2 \; I \left(\frac{p_0}{a_0}\right)^{1/2} A^{1/2}$$

where A is defined in Eq. (III.2). Because the ray tube area, A, vanishes at z = h, the integrand of Eq. (III.5) becomes infinite at that point. This singularity is integrable, however a little care is required to do it on a computer. First the integrand in Eq. (III.5) is written

$$\frac{1}{B} \frac{ds}{dz} = \frac{Q(z)}{\sqrt{h-z}}$$

and then the integral is written

$$J = Q(z_h) \int_h^z \frac{dz}{\sqrt{h-z}} + \int_h^z \frac{Q(z) - Q(z_h)}{\sqrt{h-z}} \, dz$$

$$= -2Q(z_h)\sqrt{h-z} + \int_h^z \frac{Q(z) - Q(z_h)}{\sqrt{h-z}}\, dz \qquad \text{(III.6)}$$

By using Eq. (III.2), Eq. (3.10) of Appendix I, and the definition of B (recalling $I(z_h) = 1$)

$$Q(z_h) = -\left[\frac{\sec \nu_h}{a_h^3 p_h}\right]^{1/2} \qquad \text{(III.7)}$$

The integrand in Eq. (III.6) now vanishes at the initial point $z = z_h$.

Aircraft Lift and Volume

The main interest in this study is to determine atmospheric and acceleration effects on shock propagation. Therefore details of the aircraft lift and volume calculations are omitted. Since the theory is asymptotic in the sense that it is applicable only at sufficient distance from the aircraft, a term which gives essentially only the far field effects of lift and volume is included.

The boom due to volume, for a uniform atmophere, (see e.g., Eq. 44 of Ref. 4, Appendix I) is

$$\frac{\Delta p}{p} = \frac{(M^2-1)^{1/8}}{h^{3/4}} \cdot \left\{\int_0^{\eta_0} F(\eta)\, d\eta\right\}^{1/2} \cdot \frac{\gamma 2^{1/4}}{\sqrt{\gamma+1}} \qquad \text{(III.8)}$$

$$\text{where } F(x) = \frac{1}{2\pi} \int_0^{\eta} \frac{S''(\xi)d\xi}{\sqrt{\eta-\xi}}\, d\eta$$

If area S is normalized with respect to $(L/FR)^2$ where L = aircraft length and FR = fineness ratio = (length/max diameter), and distance, η, measured along aircraft axis is normalized with respect to L, Eq. (III.8) can be written

$$\frac{\Delta p}{p} = \frac{(M^2-1)^{1/8}}{h^{3/4}} \quad \frac{L^{3/4}\ (VF)}{FR}$$

The volume factor VF varies, approximately, from .55 to .80, depending on the aircraft considered.

For a uniform atmosphere Eq. IV. 3 reduces to (after letting $K = K_v$)

$$\left.\frac{\Delta p}{p}\right|_{\text{volume}} = \frac{K_v (M^2 - 1)^{3/8}}{\sqrt{2}\, h^{3/4} M^{3/4}} \qquad \text{(III.9)}$$

Equating the above two equations leads to

$$K_v = \frac{M^{3/4}\sqrt{2}}{(M^2 - 1)^{1/4}} \quad \frac{L^{3/4}(VF)}{FR} \qquad \text{(III.10)}$$

For lifting effects (see, e.g. Eq. (49) of Ref. 6, Appendix 1) the boom overpressure is

$$\frac{\Delta p}{p} = \frac{\gamma (M^2 - 1)^{3/8}}{2^{1/4}\sqrt{x+1}} \quad \frac{\sqrt{\cos\phi}}{h^{3/4}} \left\{ \int_0^{\eta_1} G(\eta)\, d\eta \right\}^{1/2} \qquad \text{(III.11)}$$

where

$$G(\eta) = \frac{1}{2\pi} \int_0^{\eta} \frac{S''(\xi)}{\sqrt{\eta - \xi}}\, d\xi$$

and

$$S'' = \frac{d}{d\xi} \int_{\beta_1}^{\beta_2} \frac{2\Delta p\,(\xi, \beta)}{\gamma P_h M^2}\, d\beta \quad .$$

The quantity S' is essentially loading along a spanwise strip, and the integration in Eq. (III.11) is a summation of the "loading sources". If the integrals in Eq. (III.11) are made dimensionless as follows

$$\Delta p = \frac{WT}{(WS)(WC)} \overline{\Delta p} = \frac{(\text{aircraft weight})}{(\text{wing span})(\text{wing chord})} \overline{\Delta p}$$

$$\beta = (WS)\,\overline{\beta}$$

$$\eta, \xi = (WC)\,\overline{\eta}, (WC)\,\overline{\xi} \text{ ; Eq. (III.11) can be written}$$

$$\frac{\Delta p}{p} = \frac{(M^2 - 1)^{3/8}}{Mh^{3/4}} \frac{\sqrt{\cos \phi}}{(WC)^{1/4}} \left(\frac{WT}{p_h}\right)^{1/2} (LF) \qquad \text{(III.12)}$$

The lift factor LF varies, approximately, from .5 to .6.

Equating Eq. (III.9), with K_L instead of K_v, to Eq. (III.12) leads to

$$K_L = \frac{\sqrt{2}}{M^{1/4}} \frac{(LF)}{(WC)^{1/4}} \left(\frac{WT \cos \phi}{p_h}\right)^{1/2}$$

In order to combine the lift and volume effects, it should be noted that the integrals of F and G, in Eqs. III.8 and 11, should be added and not K_L and K_v. This can be accomplished by letting

$$K = \sqrt{K_v^2 + K_L^2} \qquad \text{(III.13)}$$

$$= \left[\frac{4M^3}{M^2 - 1}\right] \sqrt{\left\{\frac{L^{3/4} \cdot VF}{FR}\right\}^2 + \cos \phi \frac{\sqrt{M^2 - 1}\,(LF)^2 \cdot wT}{M^2 \cdot p_h \cdot (wc)^{1/2}}}$$

The SBCP determines the pressure ratio across the shock by using Eq. IV.3, with K defined above. At the ground the pressure ratio across the shock is multiplied by a reflection constant, RC, which equals 1.8 – 2.0, approximately.

Shock-Ground Intersection

As indicated in Appendix 1, the origin of the ray coordinate system must move with the wind at aircraft altitude. The ray-ground intersection (x_g, y_g) are related to fixed (aircraft wind) axes through Eqs. (3.13) and (3.14) of Appendix 1:

$$
\begin{aligned}
X_g &= x_g \cos\theta - y_g \sin\theta + U_h t_g \\
Y_g &= x_g \sin\theta + y_g \cos\theta + V_h t_g \\
t_g &= \text{time for ray to reach ground} \\
V_h &= \text{headwind at aircraft altitude} \\
V_h &= \text{sidewind at aircraft altitude}
\end{aligned}
\qquad \text{(III.14)}
$$

The aircraft ground speed, V_g, is given by

$$V_g = \sqrt{(V_a - U_h)^2 + V_h^2}$$

The vertex of the shock is given by the coordinates of ray $\phi = 0$, directly below the aircraft, and other points on the shock are determined by projecting back the remaining ray-ground intersection points. Since the fixed coordinate system, to which all this is referred, is aligned with the aircraft air velocity vector and not the ground speed vector the projection is carried out as follows:

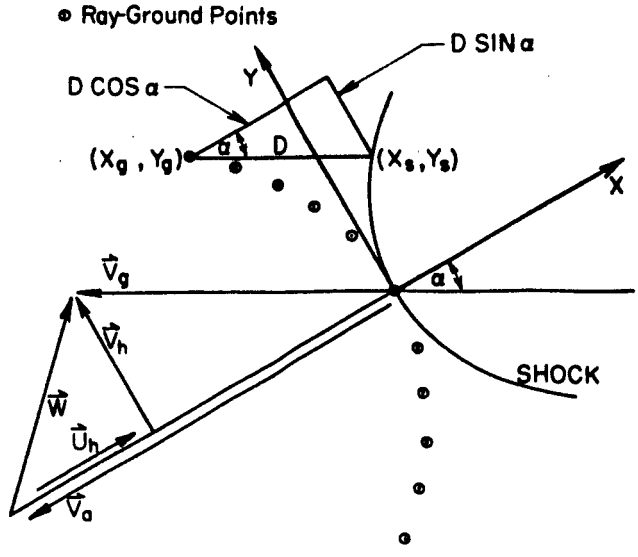

The shock maintains its shape (changes in Mach number due to acceleration are neglected) as it moves in the V_g direction. Therefore points on the shock (X_s, Y_s) are related to ray points by projecting back the distance D as indicated in Eq. (3.15) in Appendix 1. The relations are

$$X_s = X_g + D \cos \alpha$$

$$Y_s = Y_g - D \sin \alpha \qquad \text{(III.15)}$$

$$\tan \alpha = \frac{V_h}{V_a - U_h}$$

III.2 PROGRAM SYMBOLS (FORTRAN)

The altitudes are numbered: highest altitude, K = 1; lowest altitude, K = KEND = first number on control card. The atmospheric variables are

Z(1,K) = w_0, Eq. (3.2) in Appendix I

Z(2, K) = pressure, p_0

Z(3, K) = sound speed, a_0

Z(4, K) = relative wind along x axis, u_0

Z(5, K) = relative wind along y axis, v_0

Z(6, K) = I, Eq. (III.4)

Z(7, K) = altitude

Z(8, K) = aircraft headwind

Z(9, K) = aircraft sidewind

S(J), J = 1 to 9 = values of the above Z variables obtained by interpolating between two input altitudes

The angles are numbered in the order that they were entered onto the input angle cards. N = 1, corresponds to the first angle, . . . , N = NEND (second entry on control card), corresponds to the last angle. In the SBCP the angles are denoted

PHI(N) N = 1 to NEND

DATA(N,J) are output data corresponding to angle N

DATA(N,1) = pressure jump across shock

DATA(N,2) = X shock coordinate

DATA(N,3) = Y shock coordinate

DATA(N,4) = shock propagation time between aircraft and ground

W(1), Z(1), Y(1), AY(1) = parameters for evaluating Eq. (III.5)

W(2), X(2), Y(2), AY(2) = parameters for evaluating Eq. (III.1) first eqn.

W(3), X(3), Y(3), AY(3) = parameters for evaluating Eq. (III.1) second eqn.

W(4), X(4), Y(4), AY(4) = parameters for evaluating Eq. (III.1) third eqn.

W(5), X(5), Y(5), AY(5) = parameters for evaluating aircraft acceleration term in Eq. (III.2)

W(6), X(6), Y(6), AY(6) = parameters for evaluating the last integral in Eq. (III.2)

PJ(1) = altitude of point on ray path

PJ(2) = X coordinate of point on ray path

PJ(3) = Y coordinate of point on ray path

PJ(4) = shock pressure ratio of point on ray path

PJ(5) = shock pressure jump of point on ray path

PJ(6) = atmospheric pressure of point on ray path

ACC = aircraft acceleration

AF = ray tube area Eq. (III.2)

ALT = aircraft altitude

APR = previous pressure ratio

AVS = shock velocity

B = a parameter

BONG = aircraft length

BSA = aircraft lift term

BSC = aircraft shape term Eq. (III.13) without Mach number term

BSV = aircraft volume term

C = Snell's constant = $- |V_a| \cos\theta$

C1 = $V_a / (M(M^2 - 1) a_h^2)$

C2 = $BSC \cdot (4M^3/(M^2 - 1))^{.25}$

DL = integration step size

EL = ray x direction cosine

ELH = x direction cosine of ray, initially

EM = aircraft Mach number

EN = ray y direction cosine

FL = lift factor

G = $(a_h^3 p_h)^{-1/4}$ = Eq. (IV.5)

H = the negative of the y direction cosine of the ray, initially

HH = 1/H

NN = number corresponding to angle for output data

NV = number corresponding to angle $\phi = 0$

PR = pressure ratio

Q(J), J = 1, 5 = parameters

RC	=	shock-ground reflection constant
R1	=	$Q(z_a)$ in Eq. (III.7)
R2	=	$-(ds/dz)$
STH	=	$\sin\theta$
T	=	aircraft fineness ratio
TEST	=	a parameter
U	=	wind speed, u_0
VF	=	volume factor
VP	=	derivative of shock velocity
VS	=	shock velocity
WL	=	aircraft wing chord
WT	=	aircraft wieght

III.3 SUBROUTINES

In this subsection the various parts of the SBCP will be discussed. The program consists of a main part with six subroutines.

SUBROUTINE ALTA

The first subroutine encountered is called ALTA. There is a restriction on the input data, that is the aircraft altitude must be greater than the ground and less than or equal to the highest atmospheric data point. As the atmospheric data is read in by the computer, highest altitude first, they are numbered in sequential order. In subroutine ALTA the location of the aircraft altitude relative to the input altitude sequence is determined. The aircraft altitude is then made the first altitude in the sequence and all atmospheric data sequences are re-numbered starting at the aircraft altitude and going down to the ground.

SUBROUTINE ONE

In this subroutine initial conditions for all integrations and determined. Also, wind components relative to the ray coordinate system (see Appendix 1) are computed. In addition, the variable I (z) given in Eq. (III.4) is determined.

SUBROUTINE MID

All integrations are carried out by using the trapezoidal method. Some integration points fall at altitudes between the input altitudes. In subroutine MID a linear interpolation is carried out to determine atmospheric data at the points between the tabulated altitudes.

SUBROUTINE LINT

In this and the following two subroutines the integrations which are required for location of the shock and determination of the pressure jump across the shock are carried out. For the first 100 body lengths from the aircraft only the shock location is determined; some of the integrations involved in the pressure jump expression are carried out, however no shock overpressures are computed. Since the shock overpressure is not computed the true shock velocity is not known; therefore, in this initial region it is assumed that the shock propagates at acoustic speed.

The integrations over the first 100 body lengths are carried out in subroutines LINT and FIN. In LINT the integrals are evaluated by means of the trapezoidal method, with a step size equal to the spacing of input atmospheric data. This is carried out to the input altitude which is just above the altitude 100 body lengths from the aircraft.

If the aircraft altitude is the only input data point above that altitude which is 100 body lengths below the aircraft, subroutine LINT is bypassed. For this case the integration over the first 100 body lengths is carried out in subroutine FIN.

SUBROUTINE FIN

In this subroutine the shock location and overpressure integrals are evaluated between the altitude 100 body lengths from the aircraft and the input altitude immediately above it. Upon completion of this integration shock overpressure and velocity are computed for the first time.

At the end of this subroutine the step size for the remaining integrations, which continue until the ground is reached, is computed. This step size is set at one quarter of the smallest input altitude spacing.

SUBROUTINE INTEG

The shock location and overpressure integrals are determined in this subroutine using actual shock velocities. In order to do this an iteration process has been introduced, this is because the overpressure integrals is of the form.

$$p(z) = \int_h^z f(z, p(z))\, dz$$

$$\cong \int_h^{z-\Delta z} f(z, p)\, dz + \frac{\Delta z}{2} \left(f(z, p(z)) + f(z-\Delta z,\ p(z-\Delta z))\right)$$

Since the pressure at the point to be computed is on both the right and left hand sides of the above equation an iteration process is required to determine it. When two successive pressures, at a given point, agree to within one percent this value is assumed to be the correct value.

It can be shown (Ref. 10 of Appendix 1) that a more accurate expression for the ray tube area than that given in Eq. III.2 involves integrals along the shock front. A limitation of the present ray tube approach is that it assumes flow properties in each ray tube to be independent of properties in adjacent ray tubes. Therefore integrals along the shock front, through ray tubes, are not possible. The effect of these (omitted) integrals is to cause a buildup of ray tube area in opposition to a decrease in ray tube area such as would occur for an accelerating aircraft. However these integrals are only important when the shock front curvature is large, which occurs near the "cusp point" on the shock front. At this point these integrals increase in value until they cancel the aircraft acceleration term in the ray tube area expression, Eq. II.2. This behavior is taken care of in the SBCP by setting the aircraft acceleration term equal to zero at, or near the cusp point.

MAIN PROGRAM

In this part of the SBCP input, output and certain decision making operations are carried out. The most important of the decisions made is that associated with the iteration to determine the shock overpressure, described under SUBROUTINE INTEG above. This iteration is carried out

12 times. If, after this, the pressures still do not agree to within one percent the integration step size is cut in half and the procedure is started over again. This is continued, if necessary, until the integration step size is 5 feet or less. When this occurs the computation stops as there is something wrong, either with the theory, the data, or the computer.

Acoustical cutoff is assumed to occur when the shock front is within approximately 2.5 degrees of being normal to the horizontal direction. If this occurs within 100 body lengths of the aircraft, the altitude and the ray direction being considered is printed out. If cutoff occurs below 100 body lengths from the aircraft shock overpressure data is also printed out.

The last thing the program does is to compute the ground-shock data. After this is printed out the program either stops or reads in new data if there is any (last entry on control card).

SUBROUTINE CORR

Here the location of the second flight path point used for climbing or diving curved maneuvers is determined. As described in Appendix IV, this point is necessary for locating the ground-shock intersection.

SUBROUTINE SORT

In this subroutine, used only for diving and climbing flight paths, the ground-shock intersection is determined. Also, the results of the computation are printed out. The details are given in Appendix IV.

SECTION IV

IMPROVEMENTS TO THE THEORY

The general theory is given in Appendix I, however, since the publication of that theory several improvements have been made. These improvements are given in this section.

IV.1 THE PRESSURE JUMP EXPRESSION

There is a certain amount of arbitrariness in the dimensional scaling of the pressure jump expression, Eq. (2.16) of Appendix I. A more detailed discussion will be given here.

Equation (2.13) of Appendix I can be written

$$L = \frac{L_0 \left\{ \int_0^s \frac{ds}{B(s)} \right\}^{1/2}}{\left\{ \int_0^{s_0} \frac{ds}{B(s)} \right\}^{1/2}} \qquad \text{(IV.1)}$$

That is $L = L_0$ when $s = s_0$. The natural initial condition, $L = 0$ at $s = 0$, is automatically taken care of by the above solution. (The differential equation for L is singular at the initial point, hence the initial point cannot be used to prescribe initial conditions.)

Substituting the above result into the top line of Eq. (2.14), Appendix I

$$\frac{p - p_0}{p_0} = \frac{\frac{2\gamma}{\gamma+1} L_0}{a_0 I(s) \left\{ \int_0^{s_0} \frac{ds}{B(s)} \right\}^{1/2} \left\{ \int_0^s \frac{ds}{B(s)} \right\}^{1/2} \left\{ \frac{Ap}{a_0} \right\}^{1/2}} \qquad \text{(IV.2)}$$

To determine L_0 we assume a uniform atmosphere and equate Eq. (IV.2) to Eq. (2.15), Appendix I

$$\frac{2\gamma}{\gamma+1} L_0 = \frac{K}{a_0} \left\{ \int_0^{s_0} \frac{ds}{\sqrt{A}} \right\}^{1/2}$$

Therefore

$$\frac{p - p_0}{p_0} = \frac{K}{G(s_0)\, a_0^2\, I(s) \left\{ \frac{Ap}{a_0} \right\}^{1/2} \left\{ \int_0^s \frac{ds}{B(s)} \right\}^{1/2}} \quad , \qquad \text{(IV.3)}$$

where

$$G(s_0) = \left[\frac{\int_0^{s_0} \frac{ds}{B(s)}}{\int_0^{s_0} \frac{ds}{\sqrt{A}}} \right]^{1/2}$$

It should be noted that $G(s_0)$ depends on the quantity s_0 which has not yet been determined. By letting

$$\sigma = \int_0^s \frac{ds}{\sqrt{A}} \quad , \quad d\sigma = \frac{ds}{\sqrt{A}}$$

we have

$$G(\sigma_0) = \left\{ \frac{1}{\sigma_0} \int_0^{\sigma_0} \frac{d\sigma}{(a_0 + w_0)^2 I \{ p/a_0 \}^{1/2}} \right\}^{1/2} \qquad \text{(IV.4)}$$

$$= \left\{ \text{average over distance } \sigma_0 \right\}^{1/2}$$

By letting σ_0 approach zero, or the aircraft altitude, $w_0 = 0$, $I = 1$, we obtain

$$G \equiv G(0) = 1/(a_h^3\, p_h)^{1/4} \qquad \text{(IV.5)}$$

It has been found that using the value of G given in Eq. (IV.5) leads to good agreement with field test data. Therefore, Eq. (IV. 3) has been used in the SBCP with $G(s_0)$ defined in Eq. (IV.5).

By using the approach described in this section, one need not start off with dimensionless variables, as described below Eq. (2.1), Appendix 1.

IV.2 RAY TUBE AREA

The derivation of an expression for the ray tube area, given in Part 4 of Appendix 1, has been improved. It was found that Eq. (4.4) was too crude and a better approximation is given below

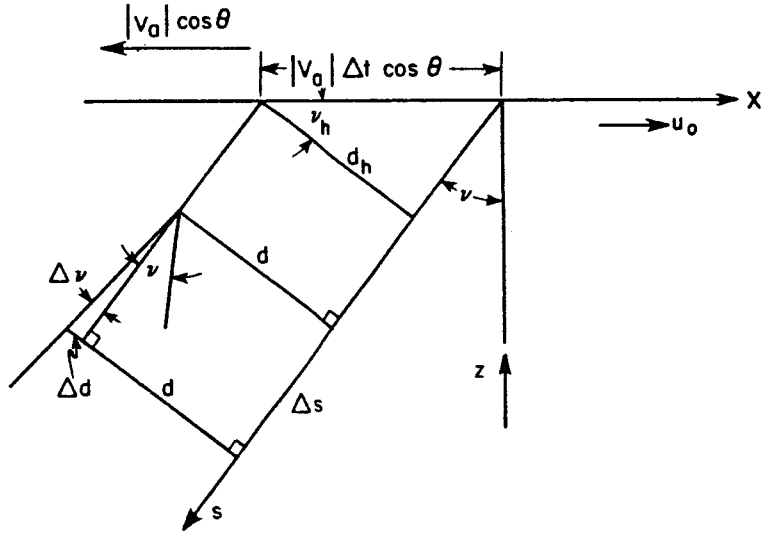

The change in distance between rays, Δd, due to a change in slope, $\Delta\nu$, in a distance Δs along the ray is

$$\Delta d = \Delta\nu \Delta s$$

Integrating this along the ray

$$d = d_h + \int_0^s \Delta\nu \, ds \tag{IV.6}$$

where $d_h = |V_a| \Delta t \cos\theta \cos\nu_h$ (IV.7)

The quantity $\Delta\nu$ will be considered to be made up of two parts

$$\Delta\nu = \Delta_1 \nu + \Delta_2 \nu \tag{IV.8}$$

The first part, $\Delta_1 \nu$, is the initial difference between the slope of the two rays caused by aircraft acceleration. The second part, $\Delta_2 \nu$, is a change

in slope due to the interrelation between the shock strength and ray tube area.

Using Eq. (3.9) of Appendix 1, at the aircraft altitude, assuming $V_s = a_h$

$$\sin \nu = \frac{a_h}{V_a \cos \theta} ,$$

and hence

$$\Delta_1 \nu = - \Delta V_a \frac{\cos \phi \cos \theta}{a_h M \sqrt{M^2 - 1}} \qquad \text{(IV.9)}$$

Variations along the ray are given by $\Delta_2 \nu$, this is determined from

$$\sin \nu = \frac{V_s}{V_a \cos \theta + u_0}$$

and leads to

$$\Delta_2 \nu = \tan \nu \left[\frac{\Delta V_s}{V_s} - \sin \nu \frac{\Delta u_0}{V_s} \right] \qquad \text{(IV.10)}$$

As in Appendix 1, Part 4, we let

$$A \sim z d \qquad \text{(IV.11)}$$

Combining Eqs. (IV.6 – 11), we obtain after some algebraic simplification of the acceleration term

$$A = z \sec \nu_h \left\{ 1 - \frac{\dot{V}_a S}{a_h^2 M (M^2 - 1)} + \frac{\sec \nu_h}{V_a \cos \theta} \int_0^S \frac{\tan \nu}{V_s} \left[\frac{dV_s}{dt} - \sin \nu \frac{du_0}{dt} \right] ds \right\} \qquad \text{(IV.12)}$$

Actually, a different approach based on the theory given in Ref. 10 of Appendix 1 will give a more correct result. However because of the complexity of that approach it is felt that its inclusion is not justified at this time. An attempt is now being made to simplify this theory in order to incorporate it into the present ray tube approach.

APPENDIX I *

EFFECTS OF ATMOSPHERE AND AIRCRAFT MOTION ON THE LOCATION AND INTENSITY OF A SONIC BOOM

In the present paper the problem of a shock propagating through a variable atmosphere is considered, and a rather complete treatment is presented. Techniques are given which permit the calculation of shock strength and location as a function of its initial configuration, the atmosphere through which it has propagated, and the distance it traveled. A specific application of this theory is made in considering the "sonic boom" caused by a supersonic aircraft. Problems such as complete acoustic refraction and/or accelerating aircraft, which give rise to shock configurations that are concave to the direction of propagation, are discussed. Attempts at solving these problems by acoustic techniques sometimes lead to physically unrealistic situations involving cusped shocks of high intensity. It is shown that when an approximation, better than the acoustic one, is used these difficulties are resolved.

Nomenclature

a = sound speed
$A(s)$ = ray-tube cross-section area
$B(s)$ = $(a_0 + w_0)^2 I(s) \{A p_0/a_0\}^{1/2}$
c = Snell's constant
e = projected aircraft travel distance, in time Δt, along x axis
$E(s)$ = ray-tube energy-source term
$G(s)$ = gravity component along ray tube
h = altitude
$I(s)$ = $\exp\left\{\int_0^s \frac{w_{0s}\rho_0 - [(\gamma-1)/2]w_0\rho_{0s}}{\rho_0(w_0+a_0)}ds\right\}$
l = wave-front normal, x direction cosine
L = correction for wave-front position
m = wave-front normal, y direction cosine
M = Mach number
$M(s)$ = ray-tube mass-source term
n = wave-front normal, z direction cosine
$n_{i,j,k}$ = direction cosines of wave-front normal
ΔN = perpendicular distance between wave-front surfaces
Q = $(\phi_{x_j}{}^2)^{1/2}$
p = pressure
r = radial distance
R = body-shape factor
s = distance along ray
$S(\eta)$ = cross-section area of aircraft
t = time
t_0 = time for vertex ray to reach ground
U = wind speed in X direction
u = wind speed in x direction
u_0 = wind speed in x direction relative to speed at aircraft altitude
V = wind speed in Y direction
v = wind speed in y direction
v_0 = wind speed in y direction relative to speed at aircraft altitude
V_a = aircraft air speed
V_g = aircraft ground speed
V_s = shock speed
w = particle velocity along ray
x = ray coordinate
X = axis along direction of aircraft motion, moving with wind at aircraft altitude
X_f = axis along direction of aircraft motion, fixed
y = ray coordinate
Y = horizontal axis perpendicular to X, moving with wind at aircraft altitude
Y_f = horizontal axis perpendicular to X, fixed
z = vertical axis
Z = vertical axis, moving with wind at aircraft altitude
Z_f = vertical axis, fixed
γ = ratio of specific heats
λ = initial angle between wave front normal and x axis
μ = Mach angle
ν = angle between shock front and x axis
ϕ = position of wave front in space and time
Φ = angular measurement about aircraft axis
ρ = density
σ = position of shock front in space
θ = angle between x and X axes
ξ,η = distance along aircraft axis, measured from nose
η_0 = point on aircraft axis where last characteristic of expansion fan behind the shock leaves the body

Subscripts

f = fixed coordinate system
h = evaluated at initial, aircraft, altitude h
i,j,k = components in (i,j,k) direction
ph = physical variable, with dimensions
0 = atmospheric condition, lowest-order perturbation
1,2 = first-, second-order perturbation

1. Introduction

A RATHER complete treatment of the sonic boom propagation problem will be presented in this paper. First, techniques will be given permitting shock-strength determination as a function of aircraft shape, altitude, Mach number, and atmospheric wind temperature and pressure variations. The shock-strength evaluation is based on a generalization of geometric acoustic ray-tube area concepts. Next, the acoustic ray-tracing equations are extended to describe shock propagation, and a method for determining the shock-ground intersection is given. Techniques developed are general enough that problems such as complete acoustic refraction and accelerating supersonic aircraft can be treated.

* The following is a reproduction of an article which appeared in AIAA Journal, Vol. 1, No. 6, June 1963, p. 1327.

The first of these problems, complete acoustic refraction, occurs when a downward moving ray is refracted upward by atmospheric variations. At the point of horizontal slope, the wave front (normal to the ray) has a cusped shape, and two adjacent rays will cross. Attempts[1-3] at describing this situation by means completely dependent on acoustics can lead to some physically unrealistic results. Geometrical acoustic theory, which describes the wave amplitude (or shock strength) as being inversely proportional to the square root of the ray-tube cross-section area, will predict an infinite amplitude at points where rays cross, corresponding to zero-tube area. This is a physically unrealistic result; in fact, the use of acoustic theory which is predicated on small amplitude perturbations is highly questionable for this situation.

The second problem concerns the wave front caused by an accelerating supersonic aircraft. For this case acoustic theory shows the wave front to be concave to its direction of propagation and the rays, if extended far enough, to intersect. At the point of intersection, cusped shocks of infinite strength are predicted.[7, 8] The foregoing comments on the acoustic refraction problem, apply equally to this problem.

The key to handling both these problems is in treatment of the ray-tube area. Acoustic approaches always have the front propagating at local sound speed and the rays dependent on ambient atmospheric conditions. For the present approach the front propagates at shock speed, and a relation between the rays and the shock strength is obtained. By means of this relation it is shown that an increase in shock strength will cause the ray tube to diverge; this diverging, in turn, will inhibit further increases in strength until finally an equilibrium configuration is attained.

Whitham[4, 5] developed a theory, for describing real shock propagation, which includes first-order acoustic terms and second-order nonlinear terms. In Whitham's and other works[6-8] based on his, the assumption had been made that the disturbances are propagating through a uniform atmosphere. This restriction will be removed, and the solution to the varying atmosphere problem will be given in Sec. 2. Expressions will be derived there which show the dependence of shock strength on atmospheric conditions and distance traveled. These results then will be combined with Whitham's to relate the shock to aircraft speed and shape.

In Sec. 3 the acoustic ray-tracing equations, which are derived in the Appendix, and their relation to the aircraft coordinate system is discussed. These equations are then altered to include true shock-propagation speeds instead of acoustic speeds. In addition, a technique is presented for determining the locus of the shock-ground intersection.

The ray-tube area is discussed in Sec. 4. An expression is developed which reduces to Whitham's[5] for steady flight in a uniform atmosphere, and which reduces to Rao's[7] for accelerating flight in a uniform atmosphere. This expression is more general than that used by either of these two authors in that it includes a term that gives the effect of shock-propagation speed on ray-tube area.

In Refs. 10 and 11, Whitham uses an expression relating shock strength (~propagation speed) and ray-tube area. He shows that converging rays, such as are associated with a concave propagating shock, will cause the ray-tube area to decrease. This decrease will in turn induce a stronger shock that propagates faster. The faster propagation of the concave part of the shock will tend to flatten the shock shape until a stable configuration is attained. Whitham's theory involves disturbances propagating along the shock front; this, however, cannot be included in the present ray-tube analysis since the basic assumption here is that the shock propagates down each tube independent of the adjoining tubes. The result of the present theory is, however, similar to Whitham's in that as the tube area decreases the shock strength will increase, which will then cause the rays to diverge. This divergence induces an increase in tube area until finally an equilibrium between the tube area and shock strength is attained.

One of the main difficulties in presenting this theory is the interdependence between the three parts of the problems; shock strength, shock location, and ray-tube area. It is hoped that the development is reasonably logical and that the cross referencing within the paper does not prove too distracting. A brief summarizing outline of the results will be given in Sec. 5.2.

2. Shock Strength

2.1 Shock Strength and Atmospheric Variations

Assume the shock is propagating through an atmosphere in which there may be pressure, density, sound speed, and wind variations with altitude but not with time. Two frames of reference will be used in this problem. The first is a moving reference frame in which the coordinate system travels with the wind at aircraft altitude. As far as the shock is concerned, its strength will be affected by the gradients of wind, temperature, and density relative to where the shock starts. Consider an aircraft moving at a given Mach number and altitude in a uniform still atmosphere and again in a uniform moving atmosphere; the strength of the shock as it reaches the ground will be the same for both cases. However, to an observer on the ground (in a fixed reference frame) the total shock distance traveled will be different. This difference is due, in the one case, to convection of the shock by the uniform wind. In computing the shock strength as a function of distance traveled one would expect that the further the shock propagates from its source, the greater will be its attenuation. However, in the problem just posed the two shocks travel different distances but still must have the same strength upon arrival at the ground. This apparent paradox is resolved by measuring shock travel distance relative to a coordinate system moving with the wind at aircraft altitude.

The second frame of reference is fixed with respect to the ground and is used only when the shock-ground intersection is computed, in Sec. 3.3. The authors therefore will assume, unless otherwise indicated, that the coordinate system is moving with the wind, and, hence, all velocities are relative to the wind velocity at aircraft altitude.

The equations for conservation of mass, momentum, and energy along a ray tube are

$$\begin{aligned} \rho_t + w\rho_s + \rho w_s + (\rho w A_s/A) &= M(s) \\ w_t + ww_s + (1/\rho)p_s &= G(s) \\ (p_t + wp_s) - (\gamma p/\rho)(\rho_t + w\rho_s) &= E(s) \end{aligned} \tag{2.1}$$

Here $\rho, w, p, A = A(s), s$ are density, particle velocity along the ray, pressure, ray-tube cross-section area, and distance along the ray. $M(s)$ and $E(s)$ are mass and energy source terms, and $G(s)$ is the component of gravity along the ray. The variables are assumed to be dimensionless; their relation to physical variables is as follows:

$$s_{ph} = sh \qquad t_{ph} = ht/a_h$$

$$\rho_{ph} = \rho\rho_h \qquad w_{ph} = a_h w \qquad p_{ph} = \rho_h a_h^2 p$$

Constants ρ_h and a_h are density and sound speed evaluated at altitude h.

Within the present theory the shock propagates down a ray tube perpendicular to the sides of the tube. Hence the flow within the tube, induced by shock motion, will remain inside the tube provided there is no gradient in the cross wind; for this case mass and energy flux through a ray tube, $M(s)$ and $E(s)$ are both zero. When there is a cross wind, $M(s)$ and $E(s)$ are not zero, their form being quite complicated since they involve derivatives of the flow variables in the direction normal to the ray.

The ray-tube area term, A_s, was shown by Whitham[5] (see also Sec. 4.1) to be proportional to distance, s, along the ray

for uniform flight in a uniform atmosphere. He then generalized this definition[5] to account for an accelerating aircraft. This will be generalized still further in Sec. 4, to account for a varying atmosphere as well as aircraft acceleration.

The quantities $E(s)$ and $M(s)$ can be simplified by noting that they represent mass and energy source terms, i.e., mass and energy being convected into a ray tube by the wind. This mass and energy will consist of atmospheric plus perturbation terms. For the present theory, only the convected atmospheric terms will be included. Neglecting the convected perturbation terms is in keeping with the assumption that the propagation of the disturbance down each ray tube can be treated separately. Since there is no mass or energy created, the quantities $E(s)$ and $M(s)$ are equated to the zeroth-order [see Eqs. (2.2)] atmospheric terms on the left-hand side of Eqs. (2.1), insuring that atmospheric mass and energy are conserved.

The solution to Eqs. (2.1) will be assumed to take the form of a perturbation on atmospheric conditions:

$$\begin{aligned} p &= p_0 + p_1(t-\sigma) + p_2(t-\sigma)^2 + \dots \\ \rho &= \rho_0 + \rho_1(t-\sigma) + \rho_2(t-\sigma)^2 + \dots \\ w &= w_0 + w_1(t-\sigma) + w_2(t-\sigma)^2 + \dots \end{aligned} \tag{2.2}$$

In Eqs. (2.2) atmospheric terms are zeroth order and are assumed to depend only on distance s. The amplitudes p_1, p_2, ρ_1, etc. are to be determined; they also depend only on s. Time dependence is introduced through the function $(t-\sigma)$. The quantity σ, a function of s, is equal to s/a_0 in a uniform atmosphere; however, it is unknown in a nonuniform atmosphere. Curves $(t-\sigma) = \text{const}$ give the positions of the wave front in space. The form given in Eqs. (2.2) is valid for small values of $(t-\sigma)$, i.e., for points near the wave front (the scaling is assumed to be such that $t = 0$ corresponds to s or $\sigma = 0$).

Derivatives of the functions in Eqs. (2.2) take the following form

$$p_t = p_1 + 2p_2(t-\sigma) + \dots$$

$$p_s = p_{0s} + p_{1s}(t-\sigma) - \sigma_s[p_1 + 2p_2(t-\sigma)] + \dots \text{etc.}$$

Substituting these into the energy equation one obtains for lowest-order terms

$$w_0 p_{0s} + p_1(1 - w_0\sigma_s) - (\gamma p_0/\rho_0)[w_0\rho_{0s} + \rho_1(1 - w_0\sigma_s)] = E(s)$$

or

$$\begin{aligned} w_0[p_{0s} - (\gamma p_0/\rho_0)\rho_{0s}] &= E(s) \\ p_1 &= (\gamma p_0/\rho_0)\rho_1 \end{aligned} \tag{2.3}$$

The quantity $E(s)$ vanishes either if $w_0 = 0$ or if the atmosphere is isentropic, $p_0 \sim \rho_0^\gamma$.

Using Eqs. (2.2) and the results of Eqs. (2.3), one obtains for the mass and momentum equations, respectively, zeroth-, first-, and second-order equations:

$$\begin{aligned} w_0 p_{0s} + \gamma p_0\left(w_{0s} + w_0\frac{A_s}{A}\right) &= \frac{\gamma p_0}{\rho_0}M(s) + E(s) \\ p_1(1 - w_0\sigma_s) - \gamma p_0 w_1\sigma_s &= 0 \\ 2p_2(1 - u_0\sigma_s) - 2\gamma p_0 w_2\sigma_s + w_0 p_{1s} + \gamma p_0 w_{1s} + & \\ w_1\left[p_{0s} - p_1\sigma_s(\gamma+1) + \left(\frac{\gamma p_0 A_s}{A}\right)\right] &= \\ \frac{\gamma p_0}{\rho_0}\left(\frac{p_1}{p_0} - \frac{\rho_1}{\rho_0}\right)M(s) & \end{aligned} \tag{2.4}$$

and

$$\begin{aligned} w_0 w_{0s} + (1/\rho_0)p_{0s} &= G(s) \\ w_1(1 - w_0\sigma_s) - (p_1/\rho_0)\sigma_s &= 0 \\ 2w_2(1 - w_0\sigma_s) - (2/\rho_0)p_2\sigma_s + w_1(w_{0s} - w_1\sigma_s) + & \\ w_0 w_{1s} + (1/\rho_0)[p_{1s} - (p_1/\gamma p_0)(p_{0s} - p_1\sigma_s)] &= 0 \end{aligned} \tag{2.5}$$

The zeroth-order equation in (2.4) defines $M(s)$

$$M(s) = w_0\rho_{0s} + \rho_0 w_{0s} + w_0\rho_0 A_s/A$$

The first-order equations in (2.4) and (2.5) are homogeneous simultaneous equations for w_1 and p_1. In order to have a nonzero solution the determinant of coefficients must be zero, i.e.,

$$(\gamma p_0/\rho_0)\sigma_s^2 - (1 - w_0\sigma_s)^2 = 0 \tag{2.6}$$

or

$$\sigma_s = [\pm 1/(a_0 \pm w_0)]$$

[The first equation in (2.6) corresponds to the eikonal equation of optics.] Take the plus sign in Eqs. (2.6) since this represents outgoing waves, that is, waves propagating in the $+s$ direction. Using Eqs. (2.6) one has

$$p_1 = (\gamma p_0/a_0)w_1 \tag{2.7}$$

and, differentiating, this gives

$$p_{1s} = \frac{\gamma p_0}{a_0}w_{1s} + \frac{\gamma w_1}{a_0}\left(p_{0s} - \frac{p_0 a_{0s}}{a_0}\right) \tag{2.8}$$

The quantities p_2 and w_2 can be eliminated by multiplying the third equation in (2.5) by $\gamma p_0/a_0$, adding it to the third equation in (2.4), and using (2.6). After substitution of p_1 in terms of w_1 by using Eqs. (2.7) and (2.8), the resulting differential equation is

$$2w_{1s} + w_1\left[\frac{A_s}{A} + \frac{p_{0s}}{p_0} - \frac{a_{0s}}{a_0} + \frac{2w_{0s}\rho_0 - (\gamma-1)w_0\rho_{0s}}{\rho_0(w_0 + a_0)}\right] - \frac{(\gamma+1)w_1^2}{(w_0+a_0)^2} = 0 \tag{2.9}$$

Before integrating Eq. (2.9) some comments on the theory and results can be made. The lowest-order perturbation relation is that given in Eq. (2.7); this corresponds to acoustic or weak shock theory. The next result is obtained by omitting the nonlinear w_1^2 term in Eq. (2.9); this corresponds to the theory of geometrical acoustics which is the next order (but not nonlinear) improvement. It can be shown that this equation agrees with Eq. (56) of Ref. 9 to terms $0(w_0^2/a_0^2)$. For an isothermal atmosphere with no winds, $a_{0s} = w_0 = 0$, and Eq. (2.9) (neglecting w_1^2) integrates to $w_1(Ap_0)^{1/2} = \text{const}$. Using Eq. (2.7), this can be written in the form now commonly used to give a correction for varying atmospheric pressure to sonic boom strength estimates

$$p_1 = p_{1h}(p_0/p_{0h})^{1/2}(A_h/A)^{1/2}$$

By retaining the w_1^2 term in Eq. (2.9) an improvement to geometrical acoustics is obtained. This is the best that can be done without involving entropy losses, which are third-order perturbation effects. Equation (2.9) can be integrated after introducing the function $I(s)$, where

$$I(s) = \exp\left\{\int_0^s \frac{w_{0s}\rho_0 - [(\gamma-1)/2]w_0\rho_{0s}}{\rho_0(w_0+a_0)}\,ds\right\}$$

the resulting integral is

$$w_1 = \frac{-2\left\{\frac{a_0(s)}{A(s)p_0(s)}\right\}^{1/2}}{(\gamma+1)I(s)\int_0^s \left\{\frac{a_0(s')}{A(s')p_0(s')}\right\}^{1/2} \frac{ds'}{I(s')[w_0(s')+a_0(s')]^2}} \quad (2.10)$$

Equation (2.10) relates the perturbation strength to distance along the ray. As the shock moves from the aircraft the cumulative effect of the expansion wave behind the shock wave is felt. It is seen[4, 5] that this is what causes the attenuation represented by the integral in Eq. (2.10). The expansion wave, in turn, is dependent on body shape. In the next section the relation between shock strength and aircraft body shape will be determined.

2.2 Shock Strength and Aircraft Shape

For acoustical theory the wave-front position can be given by $t - \sigma(s) = \text{const}$; however, it is possible, within the present improved theory to obtain a better prediction of shock position. Assume the shock location along a ray can be given by $t - \sigma(s) = -L(s)$. The quantity $L(s)$ is the correction of the present theory over acoustic theory. If one lets V_s denote shock velocity

$$1/V_s = (dt/ds) = (d\sigma/ds) - (dL/ds) = [1/(a_0 + w_0)] - (dL/ds) \quad (2.11)$$

using (2.6). Another expression for V_s is obtained by using the fact that, to the present order of approximation, the shock speed is the average of the propagation speeds in front of and behind the shock:[12]

$$\begin{aligned} V_s &= \tfrac{1}{2}(w_0 + a_0 + w + a) = w_0 + a_0 + \tfrac{1}{2}(w_1 + a_1)(t - \sigma) \\ &= w_0 + a_0 - \tfrac{1}{2}(w_1 + a_1)L(s) \\ &= w_0 + a_0 - [(\gamma+1)/4]w_1 L(s) \end{aligned} \quad (2.12)$$

or

$$1/V_s = [1/(w_0 + a_0)] + [(\gamma+1)/4][w_1 L/(w_0 + a_0)^2]$$

In the foregoing equation the quantity a_1 was eliminated by using the weak shock identity [corresponding to Eq. (2.7)]:

$$a_1 = [(\gamma-1)/2]w_1$$

Equating Eqs. (2.11) and (2.12), and using Eq. (2.10)

$$2\frac{dL}{ds} = \frac{L}{B(s)\int_0^s \frac{ds}{B(s)}}$$

with

$$B(s) = (a_0 + w_0)^2 I(s)\left[\frac{A(s)p_0(s)}{a_0(s)}\right]^{1/2}$$

This is integrated to yield

$$L(s) = R\left[\int_0^s \frac{ds}{B(s)}\right]^{1/2} \qquad R = \text{const} \quad (2.13)$$

Using the first-order relations in Eqs. (2.2) and (2.7), and then substituting Eqs. (2.10) and (2.13) one obtains an expression giving the pressure jump across the shock, relative to local pressure,

$$\begin{aligned} \frac{p - p_0}{p_0} &= \frac{\gamma w_1}{a_0}(t - \sigma) = \frac{\gamma w_1}{a_0}[-L(s)] \\ &= \frac{2\gamma R/(\gamma+1)}{a_0 I(s)\left[\frac{Ap_0}{a_0}\right]^{1/2}\left[\int_0^s \frac{ds}{B(s)}\right]^{1/2}} \end{aligned} \quad (2.14)$$

The constant R, which contains the aircraft body-shape factor, is determined by comparing Eq. (2.14) to its counterpart, Eq. (13) of Ref. 5. This equation is

$$\frac{p_1 - p_0}{p_0} = \frac{K}{A^{1/2}\left(\int_0^s \frac{ds}{A^{1/2}}\right)^{1/2}} \quad (2.15)$$

Using Eqs. (54) and (13) of Ref. 5 (the γ in the former equation should be in the numerator),

$$\begin{aligned} K &= \left[\frac{4\gamma a_0}{\gamma+1}\int_0^{T_0} F(T')dT'\right]^{1/2} \\ &= \left\{\frac{4\gamma a_0}{\gamma+1}\cdot\frac{\gamma M^{2.5}}{2^{1/2}(M^2-1)^{1/2}} \times \int_0^{T_0}\frac{1}{2\pi}\int_0^{UT'}\frac{S''(\xi)d\xi}{(UT'-\xi)^{1/2}}dT'\right\}^{1/2} \\ &= \frac{2^{3/4}\gamma}{(\gamma+1)^{1/2}}\frac{M^{3/4}}{(M^2-1)^{1/4}}\left[\int_0^{\eta_0}\frac{1}{2\pi}\int_0^{\eta}\frac{S''(\xi)d\xi}{(\eta-\xi)^{1/2}}d\eta\right]^{1/2} \end{aligned}$$

Equation (2.15) was derived assuming a uniform atmosphere. To reduce the results to this case, set $p_0 = \rho_0 = a_0 = 1$ and $w_0 = 0$ on the right-hand side of Eq. (2.14), obtaining

$$[2\gamma/(\gamma+1)]R = Kh^{-3/4}$$

The factor $h^{-3/4}$ is to make the double integral dimensionless. Combining the foregoing results, one has

$$\frac{p - p_0}{p_0} = \frac{\frac{2^{3/4}\gamma}{(\gamma+1)^{1/2}}\frac{M^{3/4}}{(M^2-1)^{1/4}}\left\{\int_0^{\eta_0}\frac{1}{2\pi}\int_0^{\eta}\frac{S''(\xi)d\xi}{(\eta-\xi)^{1/2}}d\eta\right\}^{1/2}}{a_0 I(s)\left[\frac{Ap_0}{a_0}\right]^{1/2}\left[\int_0^s\frac{ds}{B(s)}\right]^{1/2}h^{3/4}} \quad (2.16)$$

Equation (2.16) gives the pressure jump across the shock, in a nonuniform atmosphere, as a function of distance traveled, aircraft shape, and atmospheric variations.

In order to determine the wind component w_0 along the ray, the position as well as the slope of the ray corresponding to distance s must be known. This will involve a simultaneous solving of the ray equations (given in the next section) and the shock-strength equation, (2.16). The exact expression for w_0 is given in Eqs. (3.2) or (3.11). However, since wind variation is small in comparison to sound-speed magnitude, a simple approximation for w_0 can be made. One could, for example, assume the ray to be a straight line from its source to its destination and then let w_0 be the wind component along this line. The ray-tube area term A is yet to be defined. This term will be discussed in Sec. 4.1.

3. Ray Tracing and Shock Location

3.1 Acoustic Equations

It will be assumed that atmospheric sound speed a_0 and the horizontal winds (u_0, v_0) in the (x,y) directions are functions of height z alone; the vertical wind component will be neglected. If the coordinate system moves with the wind at aircraft altitude and is so aligned that the normal to the wave

front is parallel to the (x,z) plane, the acoustic ray equations (derived in Appendixes A.1 and A.3) are

$$\frac{dx}{dz} = \frac{ln_0 + u_0}{na_0} \qquad \frac{dy}{dz} = \frac{v_0}{na_0} \qquad \frac{dt}{dz} = \frac{1}{na_0}$$

$$\frac{ds}{dz} = -\left[\left(\frac{dx}{dz}\right)^2 + \left(\frac{dy}{dz}\right)^2 + 1\right]^{1/2} \qquad l = \frac{a_0}{c - u_0}$$

$$n = -(1 - l^2)^{1/2} \qquad c = \frac{a_h}{l_h} \tag{3.1}$$

The wind component along the ray now can be determined,

$$w_0 = u_0\frac{dx}{ds} + v_0\frac{dy}{ds} = \left(u_0\frac{dx}{dz} + v_0\frac{dy}{dz}\right)\frac{dz}{ds}$$

$$= \frac{u_0(dx/dz) + v_0(dy/dz)}{[(dx/dz)^2 + (dy/dz)^2 + 1]^{1/2}} \tag{3.2}$$

$$= \frac{u_0ln_0 + u_0^2 + v_0^2}{[a_0^2 + u_0^2 + v_0^2 + 2u_0ln_0]^{1/2}}$$

Geometric identities will be developed now by means of which the shock and ray cone, occurring for any physical problem, will be related to the ray-tracing equations (3.1). What is required, for any selected ray, is the position of the (x,y,z) coordinates of Eqs. (3.1) relative to the (X,Y,Z) aircraft-coordinate system. The (x,y,z) shock-coordinate system has wind velocities (u_0, v_0) in the (x,y) directions; since this coordinate system moves with the wind at the aircraft altitude, the velocities (u_0,v_0) relative to the system vanish at this altitude. The air-speed vector is along the negative X axis.

It is assumed that data are desired for rays spaced at angles Φ (see Fig. 1) about the axis of rotation (X axis). The ray-cone angle ($=90° - \mu$ where μ = Mach angle) is set by the flight condition. All data are determined in terms of μ and Φ. θ is the angle the wind components must be rotated (about the Z axis) in order to be lined up with the (x,y) coordinates, to which Eqs. (3.1) refer. Also, since rotation is about the Z axis, $z = Z$.

From the definition of μ, $\tan(90° - \mu) = (M^2 - 1)^{1/2}$, hence one has, from Fig. 1,

$$S = R\sin\Phi \qquad N = R/\tan(90° - \mu) \qquad \tan\theta = S/N$$

$$\tan\theta = \tan(90° - \mu)\sin\Phi = (M^2 - 1)^{1/2}\sin\Phi$$

therefore,

$$\cos\theta = \frac{1}{[1 + (M^2 - 1)\sin^2\Phi]^{1/2}}$$

$$\sin\theta = \frac{(M^2 - 1)^{1/2}\sin\Phi}{[1 + (M^2 - 1)\sin^2\Phi]^{1/2}} \tag{3.3}$$

Let λ be the initial angle between the ray and the positive x axis; then $l_h = \cos\lambda$. The Mach number and ray angle are related to l_h as follows:

$$T = R\cos\Phi \qquad P = S/\sin\theta = R\sin\Phi/\sin\theta$$

$$\tan\lambda = T/P = \cot\Phi\sin\theta$$

$$= \cos\Phi(M^2 - 1)^{1/2}/[1 + (M^2 - 1)\sin^2\Phi]^{1/2}$$

$$l_h = \cos\lambda = (-1/M)[1 + (M^2 - 1)\sin^2\Phi]^{1/2} \tag{3.4}$$

Letting u_0 and v_0 be the relative wind components along the x and y axes, one has

$$u_0 = (U - U_h)\cos\theta + (V - V_h)\sin\theta$$

$$v_0 = -(U - U_h)\sin\theta + (V - V_h)\cos\theta \tag{3.5}$$

where $\sin\theta$ and $\cos\theta$ are given in Eqs. (3.3).

Snell's constant is

$$c = a_0/l \qquad \text{evaluated at the initial point}$$

$$= a_h/\cos\lambda = -a_hM\cos\theta \tag{3.6}$$

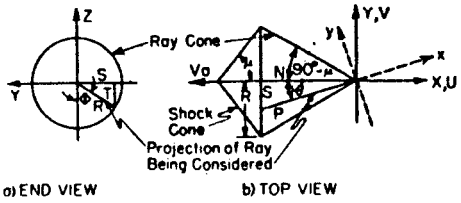

Fig. 1 Initial ray-cone coordinates

3.2 Improving the Acoustic Equations

In keeping with the theory as a whole, several parameters in Eqs. (3.1) will be improved; however, the form of the equation will be retained. First the local sound-speed term a_0 will be replaced by the shock-propagation speed V_s. This substitution can be used in both Eqs. (3.1) and (3.2).

The use of shock-propagation speed instead of sound speed leaves the derivation of Snell's law, as given in the Appendix, open to question. It will be shown now that a plane-propagating shock satisfies the same refractive law. Consider a shock propagating through a region in which atmospheric properties (Fig. 2) on either side of some horizontal line are uniform but different. The component along the x axis (Fig. 2) of the incident shock velocity relative to the wind must equal that of the refracted shock. That is both sections of the shock travel along the x axis at the same speed. Therefore,

$$(V_{1s}/\sin\nu_1) - u_1 = (V_{2s}/\sin\nu_2) - u_2 \tag{3.7}$$

This relation, which corresponds to Snell's law, will be taken to hold all along the path of shock propagation.

If one assumes now that the initial shock angle is prescribed by the Mach angle, one has, after making the identification $\sin\nu = -l$,

$$\frac{V_s}{l} + u_0 = \left(\frac{V_s}{l} + u_0\right)_{\text{initial}} = -a_hM\cos\theta$$

$$= -V_s\cos\theta \tag{3.8}$$

To obtain this relation Eqs. (3.3), (3.4) have been used, and, at the initial Mach cone, $u_h = 0$, $V_{sh} = a_h$. One sees then that, for any direction, the shock propagates at the same speed as the component of aircraft velocity in that direction. Eq. (3.8) can be derived directly from Eq. (3.6) by simply replacing sound speed by shock speed. In addition, the accuracy of Eq. (3.8) can be improved by using some of Whitham's[4] results relating the initial shock properties to the body slope at the nose.

In any case, Eq. (3.8) is of considerable importance in that it gives a relation between the ray angle and the shock velocity (or strength) V_s, as well as the ambient atmospheric and initial conditions,

$$l = \frac{-V_s}{u_0 + V_s\cos\theta} = -\sin\nu \tag{3.9}$$

This relation will be used in Sec. 4.1 for determining an expression for ray-tube area.

Equations (3.1) and (3.2) can be rewritten with shock propagation speed instead of sound speed, and with direction cosines just defined:

$$\frac{dx}{dz} = \frac{lV_s + u_0}{nV_s} \qquad \frac{dy}{dz} = \frac{v_0}{nV_s} \qquad \frac{dt}{dz} = \frac{1}{nV_s}$$

$$\frac{ds}{dz} = -\left[\left(\frac{dx}{dz}\right)^2 + \left(\frac{dy}{dz}\right)^2 + 1\right]^{1/2} \tag{3.10}$$

$$l = \frac{-V_s}{u_0 + V_s\cos\theta} = -\sin\nu \qquad n = -(1 - l^2)^{1/2} = -\cos\nu$$

$$w_0 = \frac{u_0lV_s + u_0^2 + v_0^2}{\{V_s^2 + u_0^2 + v_0^2 + 2u_0lV_s\}^{1/2}} \tag{3.11}$$

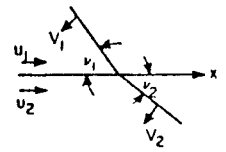

Fig. 2 Shock refraction through a nonuniform region

These equations must be integrated simultaneously with the shock strength Eq. (2.16). Equations (3.10) furnish the shock location and propagation distance s, while Eq. (2.16) furnishes the shock strength for determining V_s. Shock propagation speed is related to pressure jump as follows:

$$V_s = a_0 \left[1 + \frac{\gamma + 1}{4\gamma} \left(\frac{p - p_0}{p_0} \right) \right] \tag{3.12}$$

It should be noted that the V_s used here, and in the remainder of this paper, is different from that used in Eqs. (2.11) and (2.12). In Sec. 2, V_s represented shock velocity relative to a fixed point, $s = 0$. The V_s used here is shock-propagation speed relative to local wind. The present V_s equals the one of Sec. 2 minus w_0.

3.3 Shock-Ground Intersection

If Eqs. (3.10) are integrated from $z = 0$ to $z = -h$ (i.e., for an aircraft at altitude h) for a given angle Φ, a point on the ray-ground intersection is obtained. This must be related to a fixed coordinate system before the shock-ground locus can be constructed. Two simple transformations are required for this; the ray coordinates [Eqs. (3.10)] are related to the (X,Y,Z) coordinates by a rotation, and these coordinates are related to the fixed coordinates by a translation.

The (X,Y,Z) system initially coincides with the fixed system (X_f,Y_f,Z_f), its negative X axis aligned with the airspeed vector. For later times this system moves away from the fixed system at aircraft altitude wind speed (Fig. 3a).

These two systems are related as follows:

$$\begin{aligned} X_f &= X + U_h t \\ Y_f &= Y + V_h t \end{aligned} \tag{3.13}$$

Where t is the time taken by the selected ray to reach the ground and (U_h,V_h) are wind components along (X_f,Y_f), at the airplane altitude.

The relation between the ray system and the (X,Y,Z) system as indicated in Fig. 1b is

$$\begin{aligned} X &= x\cos\theta - y\sin\theta \\ Y &= x\sin\theta + y\cos\theta \end{aligned} \tag{3.14}$$

Equations (3.13) and (3.14), when combined, will give the locus of the ray-ground intersection. This is the locus of disturbances that left the aircraft at the same instant. What is desired, however, is the shock locus, i.e., disturbances that arrive at the ground at the same instant. This is determined easily for an aircraft flying at constant velocity, for in this case the shock locus is invariant with time. Consider first the shock and ray intersections that touch at a common vertex (Fig. 4). Points on the shock to either side of the vertex corresponds to rays that took a longer time to reach the ground. The shock moves along the ground at aircraft ground speed; a sequence of shock positions is shown in Fig. 4.

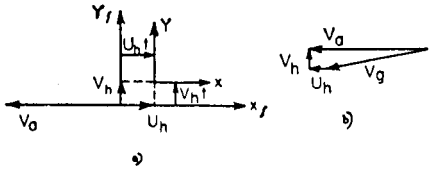

Fig. 3 a) The moving and fixed coordinate systems; b) air-speed and ground-speed vector relation

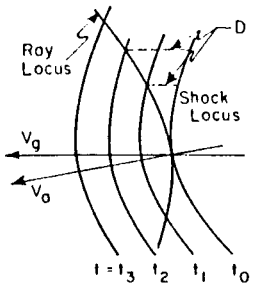

Fig. 4 Ray-shock-ground intersection. The shock is symmetric about the V_a axis but is displaced in the V_g direction

If for each point of the ray-ground intersection the distance D [Eq. (3.15) below] is projected back parallel to the ground speed direction, the corresponding point on the original $t = t_0$ shock is obtained:

$$\begin{aligned} D &= V_g(t - t_0) \\ V_g &= \text{aircraft ground speed} = [(V_a - U_h)^2 + V_h^2]^{1/2} \\ t_0 &= \text{time for vertex ray to reach ground} \\ t &= \text{time for selected ray to reach ground} \end{aligned} \tag{3.15}$$

The relation between ground speed and air speed, head wind and side wind is as indicated in Fig. 3b. Ray travel times are obtained from integration of Eqs. (3.10).

4. Ray Tube Area

4.1 Ray Distance, Atmospheric Variations, and Aircraft Acceleration

In a uniform atmosphere the shock is cone shaped, and the ray-tube cross-section area is $A = 2\pi rd$ (see Fig. 5). For the ray directly below the aircraft, $\theta = 0$ and $rd = re\cos\mu = rV_a\Delta t\cos\mu = sV_a\Delta t\cos^2\mu$; V_a = air speed, Δt = time increment, μ = Mach angle. One therefore has $A = (2\pi V_a\Delta t\cos^2\mu)s = (\text{const})\,s$ for a uniform flight speed. For this case one can replace A_s/A by $1/s$ in Eq. (2.9), or in Eqs. (2.10) and (2.16) replace A by s. With this substitution Whitham's result, Eq. (44) of Ref. 4 can be obtained.

This result now will be extended to include cases for which the atmosphere is nonuniform and the aircraft may be accelerating. The rays will not be straight lines; however, they may be described by the equation $z = x\cot\nu$, as in Fig. 6. In this equation the shock angle, ν, varies along the ray path. The distance, d, of any point (x,z) to the ray $z = x\cot\nu$ is $d = z\sin\nu - x\cos\nu$. Consider, specifically, the distance to the ray $z = (x + e)\cot(\nu + \Delta\nu)$

$$d = z[\sin\nu - \cos\nu\tan(\nu + \Delta\nu)] + e\cos\nu \tag{4.1}$$

After letting $e = V_a\cos\theta\Delta t$, where $V_a\cos\theta$ is the air-speed component along the x axis (ray-coordinate system), one can expand Eq. (4.1) in powers of $\Delta\nu$ and Δt, obtaining as first-order terms

$$d = V_a\cos\theta\Delta t\cos\nu - z\sec\nu\Delta\nu \tag{4.2}$$

The increment $\Delta\nu$ can be related to increments in shock speed, winds, and aircraft speed by using Eq. (3.9). This leads to

$$\Delta\nu = \frac{\tan\nu}{V_s} \times \left\{ \Delta V_s - \sin\nu \left[\Delta V_a\cos\theta \left(\frac{M^2\cos^2\theta - 1}{M^2 - 1} \right) + \Delta u_0 \right] \right\} \tag{4.3}$$

Using

$$\frac{\Delta V_s}{\Delta t} \approx \frac{dV_s}{dz}\frac{dz}{dt} \approx nV_s\frac{dV_s}{dz}$$

$$\frac{\Delta u_0}{\Delta t} \approx \frac{du_0}{dz}\frac{dz}{dt} \approx nV_s\frac{du_0}{dz}$$

and combining Eqs. (4.2) and (4.3), one obtains

$$d \approx \Delta t \left\{ V_s \cos\theta \cos\nu - \frac{z \tan\nu}{\cos\nu} \left[\frac{dV_s}{dz} n - \sin\nu \times \left[\frac{\cos\theta}{V_s} \frac{dV_s}{dt} \left(\frac{M^2 \cos^2\theta - 1}{M^2 - 1} \right) + \frac{du_0}{dz} n \right] \right] \right\}$$

Approximating the ray-tube area by $A = 2\pi |z| d$, and combining the equations below (4.3), one obtains finally

$$A \simeq \sec^2\nu_A |z| \left\{ \cos\nu + \frac{|z| \tan\nu}{V_s \cos\theta \cos\nu} \left[\frac{dV_s}{dz} n - \sin\nu \times \left[\frac{\cos\theta}{V_s} \frac{dV_s}{dt} \left(\frac{M^2 \cos^2\theta - 1}{M^2 - 1} \right) + n \frac{du_0}{dz} \right] \right] \right\} \quad (4.4)$$

The scaling constant, $\sec^2\nu_A$, has been inserted in order to have $A = s$ for a uniform atmosphere and flight speed.

If the aircraft is accelerating, the term dV_s/dt in Eq. (4.4) is positive. Neglecting the terms dV_s/dz and du_0/dz, one sees that for $|z|$ large enough the quantity within the braces vanishes. This gives rise to situations involving shocks of infinite amplitude as discussed by Rao.[7] In fact, if one sets

$$\theta = dV_s/dz = du_0/dz = 0$$

$$V_s = a_A = \text{sound speed at aircraft altitude}$$

$$(1/V_s)(dV_s/dt) = \dot{M}$$

$$\nu = \sin^{-1}(1/M) = \mu$$

$$z = s \cos\mu$$

one obtains Rao's result for an accelerating aircraft in a uniform atmosphere,

$$A = (\text{const}) s[1 - (s\dot{M}/M^2 \cos^2\mu V_s)]$$

For the present theory, the term dV_s/dz is crucial. By using Rao's theory, the foregoing expression implies that for a certain value of s the area vanishes and the shock amplitude is infinite. The term dV_s/dz in Eq. (4.4) prevents this from happening. This is because as the shock strength increases it propagates faster and dV_s/dz increases; it will continue increasing until it counterbalances the negative contribution from the $-dV_s/dt$ term. From then on an equilibrium shock configuration is attained as it propagates.

Ordinarily, because of the $1/V_s$, all the terms in Eq. (4.4) are negligible in comparison to $\cos\nu$, but when complete acoustic refraction occurs $\cos\nu$ goes to zero. However, before this can happen the other terms in Eq. (4.4) increase in magnitude and the ray-tube area, A, is prevented from going to zero. Again an equilibrium shock configuration is attained.

It should be noted that in the shock strength Eq. (2.16), the area term is integrated with respect to ray distance s, whereas Eq. (4.4) gives the ray-tube area as a function of z. This can be resolved by simply replacing ds, in Eq. (2.16), by $(ds/dz)dz$ and using Eqs. (3.10) to evaluate ds/dz.

In closing this section an examination of the expression for ray-tube area, Eq. (4.4), and its derivation will be made. The shock refraction Eq. (3.9) relates the local shock angle with its initial angle. Hence the terms ΔV_s and Δu_0 in Eq. (4.3) can be interpreted as contributions to the change in shock angle from its initial angle as it moves along the ray. Similarly the term ΔV_s is the contribution to the change in shock angle as the aircraft moves along the flight path. The present theory therefore considers the initial ray angle as somewhat like an equilibrium position and that changes from this position are combined with the shock-strength and location equations, in a complicated manner, to determine a new, local equilibrium configuration.

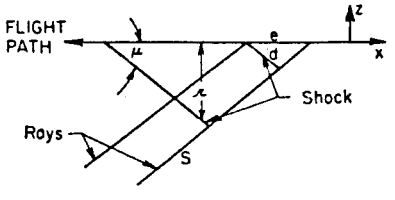

Fig. 5 Ray-tube coordinates for a uniform atmosphere

5. Conclusions and Outline

5.1 Conclusions

The present theory, when used in its total generality, requires a simultaneous solution of the shock-strength equation (2.11) and the shock-location equations (3.10) with the ray-tube area being given in Eq. (4.4). By application of this theory, sonic boom intensity and location can be determined for arbitrary aircraft and atmospheric conditions. In addition, the theory can handle problems such as complete acoustic refraction and accelerating aircraft, which are beyond the scope of acoustic approximations.

When treating any specific problem, many simplifications could be made. For example, if one considered steady flight in which no acoustic refraction occurred, the ray-tube area could be simply approximated as $A \sim s$. Also, for most cases the acoustic ray-tracing equations (3.1) probably would provide sufficiently accurate shock-location data. However, the use of Eq. (2.16) for shock-strength determination should give, in all cases, a better answer than the isothermal-pressure correction.

At the present time a digital computer program is being written to carry out computations based on the present theory. Results of these computations and the evaluation of this theory will be given in a later note.

5.2 Summarizing Outline

A brief summary of the basic assumptions and equations will be given in this section. It is assumed that the aircraft altitude, flight pattern, and the conditions of the atmosphere are known. The objective is to locate the shock-ground intersection and to determine how the shock strength varies along this intersection. First, several angular positions around the initial aircraft Mach cone are chosen. Corresponding to each of these positions a ray is located, and the ray (x,y,z) coordinate system is defined relative to the aircraft (X,Y,Z) axes. This procedure is described in Sec. 3.1. The next step is to determine the path of shock propagation, using ray-tracing equations (3.10). These equations, derived in the Appendix, are improved in Sec. 3.2 to account for actual shock propagation speed. However, in order to determine shock-propagation speeds the shock strength must be known. The variation in shock strength, as it propagates along the ray, is determined in Sec. 2 and is given in terms of pressure jump in Eq. (2.16). Propagation speed and pressure jump are related in Eq. (3.12). An important factor in determining the shock strength is the ray-tube area, and this is discussed in Sec. 4. Therefore, the ray intersection and the shock-strength variation at the ground are determined by integrating the ray-tracing equations (3.10) in conjunction with the shock-strength equations (2.16) and (3.12), and the ray-tube area equation (4.4). A technique for putting this in terms of the shock-ground intersection is given in Sec. 3.3.

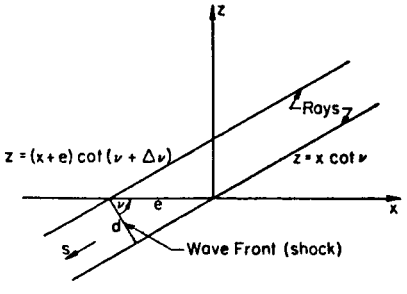

Fig. 6 Generalized ray tube coordinates

Appendix

A.1 Derivation of Acoustic Ray-Tracing Equations

All equations appearing in Secs. A.1 and A.2 are written relative to a fixed coordinate system. The transformation to the moving coordinate system, used in Sec. 3, is given in A.3. In addition, the repeated subscript summation convention will be used in order to shorten the presentation.

The equation for the acoustic wave front can be derived as a characteristic of the Eulerian flow equations. However, a simple derivation is possible if one starts with the statement: the acoustic wave front travels in a direction normal to its surface, at sound speed relative to its ambient atmosphere.

If the wave front is denoted by $\phi(x,y,z,t) = \phi(x_i,t) = 0$ the direction cosines of the normal to the front are

$$n_i = \phi_{xi}/(\phi^2_{xi})^{1/2} = \phi_{xi}/Q \tag{A1}$$

A point x_i, on the surface at time t, will at time $t + \Delta t$ be at $x_i + n_i\Delta N$, where ΔN is the perpendicular distance between the surfaces. Since x_i and $x_i + n_i\Delta N$ are on the surface

$$\phi(x_i, t) = 0 \tag{A2}$$

$$\phi(x_i + n_i\Delta N, t + \Delta t) = 0 \tag{A3}$$

Expanding Eq. (A3) in a Taylor series about the point (x_i,t) one has, after using Eq. (A2) and retaining first-order terms,

$$\Delta N n_i\phi_{xi} + \Delta t\phi_t = 0$$

Divide by Δt, and then let Δt go to zero to obtain the surface normal velocity $(dN/dt) = -(\phi_t/Q)$. The components of this velocity along the coordinate axes are

$$(dx_i/dt) = -(n_i\phi_t/Q) \tag{A4}$$

These velocity components relative to the wind components, u_i, are

$$(dx_i/dt) - u_i \tag{A5}$$

If the velocity components, Eq. (A5), are projected onto the surface normal one has, from the definition of the velocity of an acoustic wave front,

$$[(dx_i/dt) - u_i]n_i = +a \tag{A6}$$

or

$$\phi_t + u_i\phi_{xi} + aQ = 0$$

Equation (A6) describes a wave front moving through the atmosphere; one sees that the velocity components, Eq. (A5), must satisfy the relation

$$(dx_i/dt) - u_i = n_i a \qquad i = 1,2,3 \tag{A7}$$

These three equations give the velocity of a point, x_i, on the front; the locus of this point, as the surface moves through space, is called a ray. Equation (A7) shows that, if there is no wind, the ray is normal to the surface of the front. In order to solve Eqs. (A7) the direction cosines n_i must be determined. These, however, vary with the atmosphere as one moves along the ray; the differential equation for this variation will be determined now.

Letting d/dt denote differentiation along the ray one has, using Eq. (A1),

$$\frac{dn_i}{dt} = \frac{1}{Q}\frac{d}{dt}\phi_{xi} - \frac{n_i n_j}{Q}\frac{d}{dt}\phi_{xj} \tag{A8}$$

where

$$\frac{d}{dt}\phi_{xi} = \frac{\partial}{\partial t}\phi_{xi} + \frac{dx_k}{dt}\frac{\partial}{\partial x_k}\phi_{xi}$$

$$= \frac{\partial}{\partial t}\phi_{xi} + (u_k + n_k a)\frac{\partial}{\partial x_k}\phi_{xi}$$

Differentiating the second equation in (A6) are combining the result with Eq. (A8) one obtains

$$\frac{1}{n_i}\left(\frac{dn_i}{dt} + n_k\frac{\partial u_k}{\partial x_i} + \frac{\partial a}{\partial x_i}\right) = n_i n_k\frac{\partial u_k}{\partial x_j} + n_j\frac{\partial a}{\partial x_j} \tag{A9}$$

The right-hand side is independent of subscript i and is the same for each n_i, $i = 1,2,3$; therefore the differential equation for the direction cosines of the surface normal can be written as

$$\frac{1}{n_1}\left(\frac{dn_1}{dt} + n_k\frac{\partial u_k}{\partial x_1} + \frac{\partial a}{\partial x_1}\right) = \frac{1}{n_2}\left(\frac{dn_2}{dt} + n_k\frac{\partial u_k}{\partial x_2} + \frac{\partial a}{\partial x_2}\right)$$

$$= \frac{1}{n_3}\left(\frac{dn_3}{dt} + n_k\frac{\partial u_k}{\partial x_3} + \frac{\partial a}{\partial x_3}\right) \tag{A10}$$

Equations (A7), (A10), and $n_i^2 = 1$ are six equations for the six unknowns x_i,n_i along the ray.

These equations now will be simplified. First make the identification

$$(x_1,x_2,x_3,n_1,n_2,n_3) = (x,y,z;l,m,n)$$

Now assume the cross winds (u,v) and sound speed a to be dependent only on altitude z; also, vertical winds are to be neglected. The ray equations now become

$$\frac{dx}{dt} = la + u \qquad \frac{dy}{dt} = ma + v \qquad \frac{dz}{dt} = na$$

$$l^2 + m^2 + n^2 = 1 \tag{A11}$$

$$\frac{1}{l}\frac{dl}{dt} = \frac{1}{m}\frac{dm}{dt} = \frac{1}{n}\left(\frac{dn}{dt} + \frac{da}{dz} + l\frac{du}{dz} + m\frac{dv}{dz}\right)$$

From a solution of the first equality in the last equation, $l/l_h = m/m_h$ with l_h and m_h initial direction cosines. The z axis has been set as being vertical, however one is still at liberty as to the direction of the horizontal x,y axes. Let the x axis be so positioned that the normal to the wave front is parallel to the x,z plane; then $m = m_h = 0$ (The details of this coordinate positioning are given in Sec. 3.1.) Equations (A11) now read

$$\frac{dx}{dt} = la + u \qquad \frac{dy}{dt} = v \qquad \frac{dz}{dt} = na$$

$$l^2 + n^2 = 1 \qquad \frac{dl}{dt} = \frac{l}{n}\left(\frac{dn}{dt} + \frac{da}{dz} + l\frac{du}{dz}\right) \tag{A12}$$

The last three equations in (A12) can be combined to give

$$\frac{dl}{dz} = \frac{l}{a}\left(\frac{da}{dz} + l\frac{du}{dz}\right)$$

which integrates to

$$(a/l) + u = (a_h/l_h) + u_h = \text{const} \tag{A13}$$

This is Snell's law for a varying atmosphere, the right-hand side being specified by initial conditions. With Eq. (A13) and $l^2 + n^2 = 1$, one has integrated the direction-cosine equations. The ray equations are written now in their final form:

$$\frac{dx}{dz} = \frac{la + u}{na} \qquad \frac{dy}{dz} = \frac{v}{na} \qquad \frac{dt}{dz} = \frac{1}{na}$$

$$\frac{ds}{dz} = -\left[\left(\frac{dx}{dz}\right)^2 + \left(\frac{dy}{dz}\right)^2 + 1\right]^{1/2} \tag{A14}$$

$$\frac{a}{l} + u = c\ (\text{const}) \qquad l^2 + n^2 = 1$$

It is assumed that a and u are known as functions of altitude

z. Equation (A14) can be integrated from aircraft altitude to ground to give the point of intersection of the ray and the ground and the time it takes the ray to reach the ground.

A.2 Atmospheric Refraction

Complete acoustical refraction occurs when an initially downward traveling ray bends upward. The cause of this phenomenon now will be discussed. At the point of horizontal slope $n = 0$ and, hence,

$$(c - u)^2 - a^2 = (c - u - a)(c - u + a) = 0 \qquad \text{(A15)}$$

Assume that the ray moves downward in the negative x direction (see Fig. 5); then both l and n are negative, and the constant c is also negative, as for all practical cases $a > u$. Hence Eq. (A15) can vanish only when $c - u + a$ vanishes. Now consider the ray directly below the flight path; for this case $l_h = -\cos(90° - \mu) = -\sin\mu = -a_h/|V_a|$ where μ is Mach angle and V_a is aircraft air speed. When the above results are combined one sees that the ray will bend upward if $-|V_a| + a + (u_h - u)$ vanishes, i.e., if $a + (u_h - u)$ increases sufficiently as the ray travels downward. A headwind decreasing or sound speed increasing as the ground is approached will cause a ray to be bent upward. Conversely, tail winds decreasing groundward will bend rays downward.

A.3 Transformation to Moving Coordinate System

As mentioned at the beginning of Sec. 2, it is necessary to measure shock-travel distance and atmospheric wind variations relative to a coordinate system moving with the wind at aircraft altitude. In this section relations between the fixed coordinate system used in the prior two sections, and the moving coordinate system will be developed. In addition, ray-tracing equations, corresponding to (A12), will be derived for the moving coordinate system.

Denote the fixed system by (x_f, y_f, z_f), the moving system (x,y,z), and the wind components along the x_f, y_f axes by u_h, v_h, respectively. The two systems are related as follows:

$$\begin{aligned} x_f &= x + u_h t \\ y_f &= y + v_h t \\ z_f &= z \end{aligned} \qquad \text{(A16)}$$

Consider, now, Eqs. (A12) (a subscript f should be affixed to the coordinates appearing there) and substitute (A16):

$$\frac{dx}{dt} = la + u - u_h \qquad \frac{dy}{dt} = v - v_h \qquad \frac{dz}{dt} = na$$

$$l^2 + n^2 = 1 \qquad \frac{dl}{dt} = \frac{l}{n}\left(\frac{dn}{dt} + \frac{da}{dz} + l\frac{du}{dz}\right) \qquad \text{(A17)}$$

If one now introduces in (A17) wind components relative to the wind at aircraft altitude, u_0, v_0: $u_0 = u - u_h$; $v_0 = v + v_h$, the equation takes exactly the same form as (A12). Snell's law, (A13), can be written as

$$(a/l) + u - u_h = (a/l) + u_0 = (a_h/l_h) = c \qquad \text{(A18)}$$

Therefore, relative to a coordinate system moving with the wind at aircraft altitude, the ray-tracing equations are as shown in Eqs. (3.1).

References

[1] Warren, C. H. E., "An estimation of the occurrence and intensity of sonic bangs," Roy. Aircraft Establ. TN Aero. 2334 (September 1954).

[2] Randall, D. G., "Methods for estimating distributions and intensities of sonic bangs," Aeronaut. Res. Council, London, R and M 3113 (August 1957).

[3] Reed, J. W. and Adams, K. G., "Sonic boom waves—calculation of atmospheric refraction," Aerospace Eng. 21, 66–69 (March 1962).

[4] Whitham, G. B., "The flow pattern of a supersonic projectile," Communs. Pure and Appl. Math. V, 301–348 (August 1952).

[5] Whitham, G. B., "On the propagation of weak shock waves," J. Fluid Mech. I, 290–318 (1956).

[6] Walkden, F., "The shock pattern of a wing-body combination, far from the flight path," Aeronaut. Quart. IX, 164–194 (May 1958).

[7] Rao, P. S., "Supersonic bangs, part I," Aeronaut. Quart. VII, 21–44 (February 1956).

[8] Rao, P. S., "Supersonic bangs, part II," Aeronaut. Quart. VII, 135–155 (May 1956).

[9] Keller, J. B., "Geometrical acoustics; I. The theory of weak shock waves," J. Appl. Phys. 25, 938–953 (1954).

[10] Whitham, G. B., "A new approach to problems of shock dynamics; Part I, two-dimensional problems," J. Fluid Mech. 2, 145–171 (1957).

[11] Whitham, G. B., A new approach to problems of shock dynamics; Part II, three-dimensional problems," J. Fluid Mech. 5, 369–386 (1959).

[12] Courant, R. and Friedrichs, K. O., *Supersonic Flow and Shock Waves* (Interscience Publishers, Inc., New York, 1948), p. 159.

APPENDIX II
TWO SAMPLE PROBLEMS

In this section the input and output for two sample problems will be given. The first problem, case 1001, involves a low Mach number (M = 1.1) aircraft flying at 40,000 ft. and accelerating at 4 ft./sec^2; the atmosphere is an ICAO 1959 standard atmosphere. The second problem, case 0000, has a Mach 2 aircraft flying at 60,000 ft. in a constant atmosphere. The input cards for both problems are indicated as follows:

A: control card
B: atmosphere cards
C: angle card
D: aircraft data cards

Because of atmospheric refraction due to changes in temperature with altitude, the shock does not get to the ground in case 1001. There are, however, quite a few interesting results. The acceleration causes a peak overpressure at 16650 feet for the zero angle ray. This phenomenon occurs at similar altitudes for the other angle rays.

```
      16          7       1001          4          4   } A
70.          93.672     -69.61
65.          118.93     -69.61
60.          151.03     -69.61
55.          191.80     -69.61
50.          243.61     -69.61
45.          309.45     -69.61
40.          393.12     -69.61
35.          499.34     -65.52
30.          629.66     -47.74                          } B
25.          786.33     -29.96
20.          973.27     -12.17
15.          1194.8      5.63
10.          1455.6      23.44
 5.          1760.9      41.26
 1.          2040.9       55.43
 0.          2116.2      59.09
   -45.       -30.       -15.        0.        15.       30.       45.   } C
4.0          100.0        1.8       1.1       40000.     .64        .6   } D
 100000.       8.         50.
       3           4        0000          2          1         -1        } A
 60.          657.6        -44.4
  8.          657.6        -44.4                       } B
  0.          657.6        -44.4
 -30.        0.          15.          30.  } C
  0.          100.         1.8        2.0       60000.     .64        0.
 100000.       8.         50.                                              } D
```

SONIC BOOM, CASE 1001, M= 1.100, ALTITUDE= 40000., ACC= 4.000, RC=1.80, VF= 0.640, LF= 0.600
WT= 100000.0, LENGTH= 100.0, FR= 8.00, WL=50.000

ALTITUDE (FT)	HEADWIND (FPS)	SIDEWIND (FPS)	PRESSURE (PSF)	SOUND SPEED (FPS)	TEMPERATURE (DEG F)
70000.	-0.	-0.	93.672	967.660	-69.610
65000.	-0.	-0.	118.930	967.660	-69.610
60000.	-0.	-0.	151.030	967.660	-69.610
55000.	-0.	-0.	191.800	967.660	-69.610
50000.	-0.	-0.	243.610	967.660	-69.610
45000.	-0.	-0.	309.450	967.660	-69.610
40000.	-0.	-0.	393.120	967.660	-69.610
35000.	-0.	-0.	499.340	972.721	-65.520
30000.	-0.	-0.	629.660	994.422	-47.740
25000.	-0.	-0.	786.330	1015.660	-29.960
20000.	-0.	-0.	973.270	1036.475	-12.170
15000.	-0.	-0.	1194.800	1056.890	5.630
10000.	-0.	-0.	1455.600	1076.930	23.440
5000.	-0.	-0.	1760.900	1096.615	41.260
1000.	-0.	-0.	2040.900	1112.019	55.430
0.	-0.	-0.	2116.200	1115.964	59.090

CUTOFF ALTITUDE, ANGLE=-45.00

Z (FT)	X (FT)	Y (FT)	PRESSURE RATIO	PRESSURE JUMP (PSF)	PRESSURE (PSF)
26108.	-66218.	21457.	0.0026115	1.963	751.605

CUTOFF ALTITUDE, ANGLE=-30.00

Z (FT)	X (FT)	Y (FT)	PRESSURE RATIO	PRESSURE JUMP (PSF)	PRESSURE (PSF)
20433.	-80315.	18402.	0.0048093	4.603	957.070

CUTOFF ALTITUDE, ANGLE=-15.00

Z (FT)	X (FT)	Y (FT)	PRESSURE RATIO	PRESSURE JUMP (PSF)	PRESSURE (PSF)
15133.	-98920.	11732.	0.0003973	0.472	1188.913

HISTORY OF SHOCK STRENGTH VARIATION, ANGLE= 0.

Z (FT)	X (FT)	Y (FT)	PRESSURE RATIO	PRESSURE JUMP (PSF)	PRESSURE (PSF)
29750.	-23916.	-0.	0.0028460	1.814	637.493
29500.	-24582.	-0.	0.0028199	1.820	645.327
29250.	-25253.	-0.	0.0027816	1.817	653.160
29000.	-25929.	-0.	0.0027383	1.810	660.994
28750.	-26611.	-0.	0.0026937	1.802	668.827
28500.	-27299.	-0.	0.0026494	1.793	676.661
28250.	-27993.	-0.	0.0026064	1.784	684.494
28000.	-28693.	-0.	0.0025651	1.776	692.328
27750.	-29400.	-0.	0.0025257	1.768	700.161
27500.	-30114.	-0.	0.0024881	1.762	707.995
27250.	-30834.	-0.	0.0024525	1.756	715.828
27000.	-31562.	-0.	0.0024187	1.750	723.662
26750.	-32296.	-0.	0.0023866	1.746	731.495
26500.	-33039.	-0.	0.0023564	1.742	739.329
26250.	-33788.	-0.	0.0023278	1.739	747.162
26000.	-34546.	-0.	0.0023008	1.737	754.996
25750.	-35312.	-0.	0.0022755	1.736	762.829
25500.	-36087.	-0.	0.0022517	1.735	770.663
25250.	-36870.	-0.	0.0022295	1.736	778.496
25000.	-37661.	-0.	0.0022088	1.737	786.330
24750.	-38463.	-0.	0.0021882	1.741	795.677
24500.	-39273.	-0.	0.0021692	1.746	805.024
24250.	-40093.	-0.	0.0021517	1.752	814.371
24000.	-40923.	-0.	0.0021359	1.759	823.718
23750.	-41764.	-0.	0.0021217	1.768	833.065
23500.	-42615.	-0.	0.0021092	1.777	842.412

23250.	-43477.	-0.	0.0020984	1.787	851.759
23000.	-44351.	-0.	0.0020894	1.799	861.106
22750.	-45236.	-0.	0.0020823	1.813	870.453
22500.	-46134.	-0.	0.0020770	1.827	879.800
22250.	-47045.	-0.	0.0020739	1.844	889.147
22000.	-47970.	-0.	0.0020729	1.862	898.494
21750.	-48908.	-0.	0.0020742	1.883	907.841
21500.	-49861.	-0.	0.0020781	1.906	917.188
21250.	-50829.	-0.	0.0020849	1.932	926.535
21000.	-51814.	-0.	0.0020947	1.960	935.882
20750.	-52815.	-0.	0.0021080	1.993	945.229
20500.	-53834.	-0.	0.0021252	2.029	954.576
20250.	-54872.	-0.	0.0021471	2.070	963.923
20000.	-55929.	-0.	0.0021742	2.116	973.270
19750.	-57007.	-0.	0.0022064	2.172	984.346
19500.	-58107.	-0.	0.0022467	2.236	995.423
19250.	-59230.	-0.	0.0023083	2.323	1006.499
19000.	-60378.	-0.	0.0023645	2.406	1017.576
18750.	-61553.	-0.	0.0024559	2.526	1028.652
18500.	-62756.	-0.	0.0025621	2.664	1039.729
18250.	-63989.	-0.	0.0026971	2.834	1050.805
18000.	-65257.	-0.	0.0028764	3.054	1061.882
17750.	-66561.	-0.	0.0031440	3.373	1072.958
17700.	-66829.	-0.	0.0031561	3.393	1075.174
17650.	-67100.	-0.	0.0030880	3.327	1077.389
17600.	-67375.	-0.	0.0030795	3.325	1079.604
17550.	-67652.	-0.	0.0031048	3.359	1081.820
17500.	-67931.	-0.	0.0031507	3.416	1084.035
17450.	-68212.	-0.	0.0032105	3.487	1086.250
17400.	-68495.	-0.	0.0032966	3.588	1088.466
17350.	-68780.	-0.	0.0033649	3.670	1090.681
17300.	-69068.	-0.	0.0034656	3.788	1092.896
17250.	-69357.	-0.	0.0035475	3.885	1095.111
17200.	-69650.	-0.	0.0036691	4.026	1097.327
17150.	-69944.	-0.	0.0037871	4.164	1099.542
17100.	-70241.	-0.	0.0039142	4.313	1101.757
17050.	-70541.	-0.	0.0040545	4.476	1103.973
17000.	-70844.	-0.	0.0042101	4.657	1106.188
16950.	-71150.	-0.	0.0043828	4.858	1108.403
16900.	-71459.	-0.	0.0045746	5.081	1110.619
16850.	-71772.	-0.	0.0047874	5.328	1112.834
16800.	-72088.	-0.	0.0050230	5.601	1115.049
16750.	-72407.	-0.	0.0052827	5.902	1117.264
16700.	-72731.	-0.	0.0055668	6.232	1119.480
16650.	-73060.	-0.	0.0058748	6.590	1121.695
16600.	-73384.	-0.	0.0004907	0.552	1123.910
16550.	-73700.	-0.	0.0004897	0.551	1126.126
16500.	-74013.	-0.	0.0004884	0.551	1128.341
16250.	-75590.	-0.	0.0004832	0.551	1139.417
16000.	-77207.	-0.	0.0004763	0.548	1150.494
15750.	-78879.	-0.	0.0004687	0.544	1161.570
15500.	-80623.	-0.	0.0004607	0.540	1172.647
15250.	-82452.	-0.	0.0004526	0.536	1183.723
15000.	-84383.	-0.	0.0004444	0.531	1194.800
14750.	-86435.	-0.	0.0004360	0.527	1207.840
14500.	-88635.	-0.	0.0004275	0.522	1220.880
14250.	-91019.	-0.	0.0004169	0.514	1233.920
14000.	-93642.	-0.	0.0004094	0.510	1246.960
13750.	-96596.	-0.	0.0004012	0.506	1260.000
13500.	-100051.	-0.	0.0003903	0.497	1273.040
13250.	-104416.	-0.	0.0003819	0.491	1286.080

CUTOFF ALTITUDE, ANGLE= 0.

Z (FT)	X (FT)	Y (FT)	PRESSURE RATIO	PRESSURE JUMP (PSF)	PRESSURE (PSF)
13242.	-104572.	-0.	0.0003773	0.485	1286.487

CUTOFF ALTITUDE, ANGLE= 15.00

Z (FT)	X (FT)	Y (FT)	PRESSURE RATIO	PRESSURE JUMP (PSF)	PRESSURE (PSF)
15133.	-98921.	-11733.	0.0003972	0.472	1188.913

CUTOFF ALTITUDE, ANGLE= 30.00

Z (FT)	X (FT)	Y (FT)	PRESSURE RATIO	PRESSURE JUMP (PSF)	PRESSURE (PSF)
20433.	-80314.	-18402.	0.0048083	4.602	957.070

CUTOFF ALTITUDE, ANGLE= 45.00

Z (FT)	X (FT)	Y (FT)	PRESSURE RATIO	PRESSURE JUMP (PSF)	PRESSURE (PSF)
26108.	-66215.	-21456.	0.0026088	1.961	751.605

SONIC BOOM, CASE 1001, M= 1.100, ALTITUDE= 40000.

SHOCK-GROUND DATA

ANGLE (DEG)	PRESSURE JUMP (PSF)	X (FT)	Y (FT)	TIME (SEC)
-45.00	0.	0.	0.	-1.00
-30.00	0.	0.	0.	-1.00
-15.00	0.	0.	0.	-1.00
0.	0.	0.	0.	-1.00
15.00	0.	0.	0.	-1.00
30.00	0.	0.	0.	-1.00
45.00	0.	0.	0.	-1.00

SONIC BOOM, CASE 0, M= 2.000, ALTITUDE= 60000., ACC= 0. , RC=1.80, VF= 0.640, LF= 0.
WT= 100000.0, LENGTH= 100.0, FR= 8.00, WL=50.000

ALTITUDE (FT)	HEADWIND (FPS)	SIDEWIND (FPS)	PRESSURE (PSF)	SOUND SPEED (FPS)	TEMPERATURE (DEG F)
60000.	-0.	-0.	657.600	998.446	-44.400
8000.	-0.	-0.	657.600	998.446	-44.400
0.	-0.	-0.	657.600	998.446	-44.400

HISTORY OF SHOCK STRENGTH VARIATION, ANGLE=-30.00

Z (FT)	X (FT)	Y (FT)	PRESSURE RATIO	PRESSURE JUMP (PSF)	PRESSURE (PSF)
49340.	-7108.	6156.	0.0024984	1.643	657.600
47340.	-8444.	7313.	0.0022029	1.449	657.600
45340.	-9780.	8470.	0.0019716	1.297	657.600
43340.	-11116.	9626.	0.0017893	1.177	657.600
41340.	-12451.	10783.	0.0016420	1.080	657.600
39340.	-13786.	11939.	0.0015202	1.000	657.600
37340.	-15121.	13095.	0.0014176	0.932	657.600
35340.	-16456.	14251.	0.0013362	0.879	657.600
33340.	-17790.	15407.	0.0012609	0.829	657.600
31340.	-19125.	16563.	0.0011938	0.785	657.600
29340.	-20460.	17719.	0.0011342	0.746	657.600
27340.	-21794.	18874.	0.0010811	0.711	657.600
25340.	-23129.	20030.	0.0010335	0.680	657.600
23340.	-24463.	21186.	0.0009904	0.651	657.600
21340.	-25798.	22341.	0.0009514	0.626	657.600
19340.	-27132.	23497.	0.0009157	0.602	657.600
17340.	-28466.	24652.	0.0008830	0.581	657.600
15340.	-29800.	25808.	0.0008529	0.561	657.600
13340.	-31135.	26963.	0.0008252	0.543	657.600
11340.	-32469.	28119.	0.0007994	0.526	657.600
9340.	-33803.	29274.	0.0007754	0.510	657.600
7340.	-35137.	30430.	0.0007569	0.498	657.600
5340.	-36471.	31585.	0.0007331	0.482	657.600
3340.	-37805.	32740.	0.0007164	0.471	657.600
1340.	-39139.	33896.	0.0006951	0.457	657.600
0.	-40033.	34670.	0.0006844	0.450	657.600

SONIC BOOM, CASE 0, M= 2.000, ALTITUDE= 60000.

SHOCK-GROUND DATA

ANGLE (DEG)	PRESSURE JUMP (PSF)	X (FT)	Y (FT)	TIME (SEC)
-30.00	0.810	-18569.	34670.	80.12
0.	0.901	-34663.	0.	69.37
15.00	0.876	-30994.	-16088.	71.82
30.00	0.810	-18569.	-34669.	80.12

APPENDIX III

FORTRAN LISTING

```
*       SYMBOL TABLE
*        LIST8
*        LABEL
        SUBROUTINE ALTA
        DIMENSION Z(9,100),S(9),W(9),X(9),Y(9),PJ(7),Q(9),AY(9),DATA(21,5)
       1,PHI(21)
        COMMON Z,KEND,CTH,STH,C,B,S,G,KQ,DL,H,R1,W,X,C1,Y,F,VS,VP,C2,AY,PJ
       1,BSV,BSA,PHI,DATA,PR,U,AVS,JNR,NEND,ALT,EL,Q,EZ,BSC,ELH,KASE,EM,EN
       1,N,ACC,RC,BONG,NV,NN,JOBS,WT,T,WL,VF,FL,APR,BVP,TEST,AF,HH
        DO 50 K=1,KEND
        IF(ALT-Z(7,K)) 50,50,51
  50    CONTINUE
  51    KA=K
        R=(ALT-Z(7,KA))/(Z(7,KA-1)-Z(7,KA))
        DO 52 J=1,9
        Z(J,1)=Z(J,KA)+R*(Z(J,KA-1)-Z(J,KA))
        DO 53 K=KA,KEND
        KK=K-KA+2
  53    Z(J,KK)=Z(J,K)
  52    CONTINUE
        KEND=KEND-KA+2
       G=(Z(3,1)/Z(2,1))**.25/Z(3,1)
       BSV=VF/T*BONG**.75
       BSA=FL*SQRTF(WT/Z(2,1)/SQRTF(WL))
        RETURN
        END
```

```
*       LISTA
*       LABEL
*       SYMBOL TABLE
        SUBROUTINE ONE
        DIMENSION Z(9,100),S(9),W(9),X(9),Y(9),PJ(7),Q(9),AY(9),DATA(21,5)
       1,PHI(21)
        COMMON Z,KEND,CTH,STH,C,B,S,G,KQ,DL,H,R1,W,X,C1,Y,F,VS,VP,C2,AY,PJ
       1,BSV,BSA,PHI,DATA,PR,L,AVS,JNR,NEND,ALT,EL,Q,EZ,BSC,ELH,KASE,EM,EN
       1,N,ACC,RC,BONG,NV,NN,JOBS,WT,T,WL,VF,FL,APR,BVP,TEST,AF,HH
        EZ=0.
        B=EM*EM-1.
        DQ=COSF(PHI(N)/57.2958)
        BSC=SQRTF(BSV*BSV+DQ*BSA*BSA*SQRTF(B)/(B+1.))
        D=SINF(PHI(N)/57.2958)
        CTH=1./SQRTF(1.+B*D*D)
        STH=CTH*D*SQRTF(B)
        ELH=-1./(EM*CTH)
        H=SQRTF(1.-ELH*ELH)
         HH=1.0/H
        C=Z(3,1)/ELH
         C1=ACC/EM/B/Z(3,1)/Z(3,1)
        C2=1.414*BSC*(EM**3/B)**.25
   14   R1=1./(Z(3,1)**1.5*SQRTF(Z(2,1)*H))
         DO 15 M=1,6
   15    Y(M)=0.
        W(1)=0.
        W(2)=-ELH/H
        W(3)=0.
        W(4)=-1./(Z(3,1)*H)
         W(5)=C1/H/H
        Z(4,1)=0.
        Z(5,1)=0.
        Z(1,1)=0.
        Z(6,1)=1.
        DO 8 K=2,KEND
        Z(4,K)=CTH*(Z(8,K)-Z(8,1))+STH*(Z(9,K)-Z(9,1))
        Z(5,K)=CTH*(Z(9,K)-Z(9,1))-STH*(Z(8,K)-Z(8,1))
        B=Z(4,K)*Z(3,K)**2/(C-Z(4,K))
        V=Z(4,K)**2+Z(5,K)**2
        Z(1,K)=(B+V)/SQRTF(Z(3,K)**2+V+2.*B)
        DO 5 I=1,3
    5   S(I)=.5*(Z(I,K)+Z(I,K-1))
        B=Z(1,K)-Z(1,K-1)
        V=(Z(2,K)-Z(2,K-1))/S(2)
        F=2.*(Z(3,K)-Z(3,K-1))/S(3)
    8   Z(6,K)=Z(6,K-1)*EXPF((B-.2*S(1)*(V-F))/(S(1)+S(3)))
         Q(1)=(Z(3,2)+Z(1,2)-Z(3,1))/(Z(7,2)-Z(7,1))
   13    W(6)=Q(1)*ELH/C/H/H
        DO 16 KZ=1,9
   16   Q(KZ)=0.

        RETURN
        END
```

```
*       SYMBOL TABLE
*       LIST8
*       LABEL
        SUBROUTINE MID
        DIMENSION Z(9,100),S(9),W(9),X(9),Y(9),PJ(7),Q(9),AY(9),DATA(21,5)
       1,PHI(21)
        COMMON Z,KEND,CTH,STH,C,B,S,G,KQ,DL,H,R1,W,X,C1,Y,F,VS,VP,C2,AY,PJ
       1,BSV,BSA,PHI,DATA,PR,U,AVS,JNR,NEND,ALT,EL,Q,EZ,BSC,ELH,KASE,EM,EN
       1,N,ACC,RC,BONG,NV,NN,JOBS,WT,T,WL,VF,FL,APR,BVP,TEST,AF,HH
        S(7)=S(7)+DL
        IF(S(7)-Z(7,KEND)-5.)65,65,61
   65   DL=Z(7,KEND)+DL-S(7)
        S(7)=Z(7,KEND)
   61   DO 62 K=KQ,KEND
        IF(S(7)-Z(7,K))62,63,63
   62   CONTINUE
   63   KQ=K-1
        R=(S(7)-Z(7,KQ))/(Z(7,KQ+1)-Z(7,KQ))
        DO 64 J=1,6
   64   S(J)=Z(J,KQ)+R*(Z(J,KQ+1)-Z(J,KQ))
        RETURN
        END
```

```
*       SYMBOL TABLE
*       LIST8
*       LABEL
        SUBROUTINE LINT
        DIMENSION Z(9,100),S(9),W(9),X(9),Y(9),PJ(7),Q(9),AY(9),DATA(21,5)
       1,PHI(21)
        COMMON Z,KEND,CTH,STH,C,B,S,G,KQ,DL,H,R1,W,X,C1,Y,F,VS,VP,C2,AY,PJ
       1,BSV,BSA,PHI,DATA,PR,U,AVS,JNR,NEND,ALT,EL,Q,EZ,BSC,ELH,KASE,EM,EN
       1,N,ACC,RC,BONG,NV,NN,JOBS,WT,T,WL,VF,FL,APR,BVP,TEST,AF,HH
        DO 24 K=2,KQ
        EL=Z(3,K)/(C-Z(4,K))
        IF(ABSF(EL)-.999)20,21,21
   21   Q(1)=1.
        S(7)=Z(7,K)
        GO TO 23
   20   EN=-SQRTF(1.-EL*EL)
        X(4)=1./(Z(3,K)*EN)
        X(3)=Z(5,K)*X(4)
        X(2)=(EL*Z(3,K)+Z(4,K))*X(4)
        R2=SQRTF(1.+X(3)**2+X(2)**2)
        X(5)=C1*R2
         ZDL=Z(7,K)-Z(7,K-1)
         B=(Z(3,K)-Z(3,K-1))/ZDL
        BA=EL*(Z(4,K)-Z(4,K-1))/ZDL
   26   X(6)=-EL*(B+BA)/C/EN/H
         B=0.5*ZDL
         DO 22 M=2,6
        Y(M)=Y(M)+B*(W(M)+X(M))
   22   W(M)=X(M)
   25   F=(1.+Y(5)+Y(6))/H
        IF(F)27,27,29
   27   F=F-Y(5)/H
         Y(5)=0.
         W(5)=0.
         C1=0.0
         Q(2)=1.0
         Q(4)=Z(7,K)
   29   R4=R2/((Z(3,K)+Z(1,K))**2*SQRTF(F*Z(2,K)/Z(3,K))*Z(6,K))
        X(1)=(R1-R4)/SQRTF(Z(7,I)-Z(7,K))
         Y(1)=B*(W(1)+X(1))+Y(1)
         W(1)=X(1)
   24   CONTINUE
   23   RETURN
        END
```

```
*       SYMBOL TABLE
*       LIST8
*       LABEL
        SUBROUTINE FIN
        DIMENSION Z(9,100),S(9),W(9),X(9),Y(9),PJ(7),Q(9),AY(9),DATA(21,5)
       1,PHI(21)
        COMMON Z,KEND,CTH,STH,C,B,S,G,KQ,DL,H,R1,W,X,C1,Y,F,VS,VP,C2,AY,PJ
       1,BSV,BSA,PHI,DATA,PR,U,AVS,JNR,NEND,ALT,EL,G,EZ,BSC,ELH,KASE,EM,EN
       1,N,ACC,RC,BONG,NV,NN,JOBS,AT,T,WL,VF,FL,APR,BVP,TEST,AF,HH
        Y(1)=Y(1)+2.*R1*SQRTF(Z(7,1)-S(7))
        EL=S(3)/(C-S(4))
        IF(ABSF(EL)-.999)26,27,27
   27   Q(1)=1.
        GO TO 30
   26   EN=-SQRTF(1.-EL*EL)
        X(4)=1./(EN*S(3))
        X(3)=S(5)*X(4)
        X(2)=(EL*S(3)+S(4))*X(4)
        R2=SQRTF(1.+X(2)**2+X(3)**2)
         ZDL=S(7)-Z(7,KQ)
         B=(S(3)-Z(3,KQ))/ZDL
        BA=EL*(S(4)-Z(4,KQ))/ZDL
        X(5)=C1*R2
   23   X(6)=-EL*(B+BA)/C/EN/H
         B=0.5*ZDL
         DO 25 M=2,6
        Y(M)=Y(M)+B*(X(M)+W(M))
   25   W(M)=X(M)
   24   F=(1.+Y(5)+Y(6))/H
         IF(F) 34,34,37
   34   F=F-Y(5)/H
        C1=0.
        Q(2)=1.
         Y(5)=0.0
         W(5)=0.0
         GO TO 37
   37   R4=R2/((S(3)+S(1))**2*S(6)*SQRTF(F*S(2)/S(3)))
        X(1)=(R1-R4)/SQRTF(Z(7,1)-S(7))
         Y(1)=B*(W(1)+X(1))+Y(1)
         W(1)=X(1)
        W(1)=W(1)-R1/SQRTF(Z(7,1)-S(7))
   28   DL=Z(7,KQ)
        KL=KEND-1
        DO 35 K=KQ,KL
        B=Z(7,K)-Z(7,K+1)
   35   DL=MIN1F(DL,B)
        DL=-.25*DL
   29   B=G*S(6)*S(3)*S(3)
        HA=SQRTF(Y(1)*S(2)*F*(Z(7,1)-S(7))/S(3))
        PR=C2/B/HA
        VS=S(3)*(1.+.4286*PR)
       VP=(VS-S(3))/DL
   33   F=F*(Z(7,1)-S(7))
   30   RETURN
        END
```

```
*       LISTP
*       LABEL
*       SYMBOL TABLE
        SUBROUTINE INTEG
        DIMENSION Z(9,100),S(9),W(9),X(9),Y(9),PJ(7),Q(9),AY(9),DATA(21,5)
       1,PHI(21)
        COMMON Z,KEND,CTH,STH,C,B,S,G,KQ,DL,H,R1,W,X,C1,Y,F,VS,VP,C2,AY,PJ
       1,BSV,BSA,PHI,DATA,PR,U,AVS,JNR,NEND,ALT,EL,Q,EZ,BSC,ELH,KASE,EM,EN
       1,N,ACC,RC,BONG,NV,NN,JOBS,WT,T,WL,VF,FL,APR,BVP,TEST,AF,HH
 41    FL=-VS/(S(4)-C)
       IF(ABSF(EL)-.999)415,43,43
   43  Q(1)=1.
       GO TO 49
 415   EN=-SQRTF(1.-EL*FL)
       X(4)=1./EN/VS
       X(2)=(EL*VS+S(4))*X(4)
       X(3)=S(5)*X(4)
       R2=SQRTF(1.+X(2)**2+X(3)**2)
       B1=(S(4)-U)*EL/DL
       X(5)=C1*R2
   44  X(6)=-EL*(VP+B1)/C/EN/H
        B=0.5*DL
        DO 42 M=2,6
 42    AY(M)=Y(M)+B*(W(M)+X(M))
       AF=1.+AY(5)+AY(6)
       IF(AF-.01)48,417,417
 48     AF=AF-AY(5)
       C1=0.
        AY(5)=0.0
        Y(5)=0.0
        W(5)=0.0
       Q(5)=3.
 417   F=(Z(7,1)-S(7))*AF/H
 416   X(1)=R2/S(6)/((S(3)+S(1))**2*SQRTF(S(2)*F/S(3)))
       X(1)=-X(1)
        AY(1)=Y(1)+B*(W(1)+X(1))
       B=G*S(6)*S(3)**2
       PR=.5*(C2/B/SQRTF(AY(1)*S(2)*F/S(3))+APR)
       VS=.5*(AVS+S(3)*(1.+.4286*PR))
        VP=(VS-AVS)/DL
   49  RETURN
       END
```

```
*       LABEL
*       SYMBOL TABLE
CSBOOM
        DIMENSION Z(9,100),S(9),W(9),X(9),Y(9),PJ(7),Q(9),AY(9),DATA(21,5,
       1 2),PHI(21)
        COMMON Z,KEND,CTH,STH,C,B,S,G,KQ,DL,H,R1,W,X,C1,Y,F,VS,VP,C2,AY,PJ
       1,BSV,BSA,PHI,DATA,PR,U,AVS,JNR,NEND,ALT,EL,Q,EZ,BSC,ELH,KASE,EM,EN
       1,N,ACC,RC,BONG,NV,NN,JOBS,WT,T,WL,VF,FL,APR,BVP,TEST,AF,HH
         COMMON CRV,PSI,TAU, PS,TS,XD,YD,ZD ,VT,MP
  310  READ 200,KEND,NEND,KASE,NV,NN,JOBS
        READ 201,(Z(7,K),Z(2,K),Z(1,K),Z(8,K),Z(9,K),K=1,KEND)
        READ 202,(PHI(N),N=1,NEND)
        READ 202,ACC,BONG,RC,EM,ALT,VF,FL,WT,T,WL,CRV,PSI,TAU
         UM=ASINF(1.0/EM) *57.2958
         IF (90.0-UM-PSI) 11,11,13
  11     PRINT 204,KASE,EM,ALT
         PRINT 218
  218    FORMAT (39HONO SHOCKS AT GROUND DUE TO CLIMB ANGLE)
         GO TO 38
  13    B=(ALT-100.*BONG)/1000.
        IF(B-Z(7,KEND))12,12,39
    12   PRINT 204, KASE,EM,ALT
        PRINT 213
        GO TO 38
    39  DO 112 K=1,KEND
        Z(7,K)=Z(7,K)*1000.
   112  Z(3,K)=49.*SQRTF(Z(1,K)+459.6)
     2  PRINT 205,KASE,EM,ALT,ACC,RC,VF,FL,WT,BONG,T,WL  ,PSI,TAU,CRV
        PRINT 206
         PRINT 207,(Z(7,K),Z(8,K),Z(9,K),Z(2,K),Z(3,K),Z(1,K),K=1,KEND)
         DVC=0.0
         MP=1
         IF (ABSF(PSI) + ABSF(CRV)) 40,40,41
  41     DVC=1.0
         CALL CORR
  40    CALL ALTA
  1     DO 111 N=1,NEND
        N=N
        DO 5 J=1,5
    5   DATA(N,J,MP)=0.
        CALL ONE
        S(7)=Z(7,1)-100.*BONG*COSF(PHI(N)/57.3)
C       ACOUSTIC INITIAL INTEGRATION
  14    KQ=1
        DL=0.
        CALL MID
        IF(KQ-1)18,18,19
  19    CALL LINT
        IF(Q(2)-1.)25,23,25
    23  Q(2)=0.
        PRINT 216,Q(4),PHI(N)
    25  IF(Q(1)-1.)18,21,18
  18    CALL FIN
        IF(Q(2)-1.)22,24,22
    24  Q(2)=0.
        PRINT 216,S(7),PHI(N)
    22  IF(Q(1)-1.)20,21,20
    21  PRINT 215,S(7),PHI(N)
        GO TO 111
C       SHOCK INTEGRATION STARTS HERE
    20  ADL=.75*DL
```

```
      DLT=DL
   80 U=S(4)
      AVS=VS
      BVP=VP
   81 CALL MID
   99 TEST=-2.
   85 CALL INTEG
   98 IF(Q(1)-1.)3,4,3
    4 Q(1)=0.
      IF (DL+10.0) 78,31,31
    3 IF(TEST+1.)82,83,83
   82 TEST=TEST+1.
      APR=PR
      GO TO 85
   83 V=2.*ABSF(PR-APR)/(PR+APR)
      IF(V-.01)86,86,87
   87 TEST=TEST+1.
      APR=PR
      IF(TEST-10.0) 85,85,88
   88 IF(DL+5.)78,77,77
   78 S(7)=S(7)-DL
      DL=.5*DL
   96 VS=AVS
      VP=BVP
      GO TO 81
   77 PRINT 217,PHI(N)
      GO TO 91
   31 PRINT 214,PHI(N)
   91 PRINT 211
      DATA(N,4,MP)=-1.0
      GO TO 90
   86 IF(NN-N)89,37,89
   37 IF (DVC-1.0) 45,45,89
   45 IF (EZ) 36,36,90
   36 EZ=1.
      PRINT 210,(PHI(NN))
      PRINT 211
   90 PJ(6)=S(2)
      PJ(4)=PR
      PJ(5)=S(2)*PR
      PJ(1)=S(7)
      PJ(3)=   AY(3)*CTH+AY(2)*STH+AY(4)*Z(9,1)
      PJ(2)=   AY(2)*CTH-AY(3)*STH+AY(4)*Z(8,1)
      PRINT 212,(PJ(I),I=1,6)
      IF (DATA(N,4,MP)) 111,89,89
   89 DO 71 M=1,6
      W(M)=X(M)
   71 Y(M)=AY(M)
      IF(DL+10.)72,76,76
   76 DL=ADL
   72 IF(S(7)-Z(7,KEND))70,70,95
   95 IF (Q(5)-1.0) 92,93,94
   92 IF (AF-0.05) 97,97,80
   97 DL=MAX1F(-50.0,DL)
      GO TO 80
   94 Q(5)=Q(5)-1.
      GO TO 80
   93 DL=DLT
      Q(5)=0.0
```

```
      GO TO 80
   70  DATA(N,1,MP)=RC*Z(2,KEND)*PR
       DATA(N,4 ,MP)=Y(4)
       DATA(N,3,MP)=Y(4)*Z(9,1)+Y(2)*STH+Y(3)*CTH
       DATA(N,2,MP)=Y(2)*CTH-Y(3)*STH+Y(4)*Z(8,1)
  111  CONTINUE
       IF (DVC-1.0) 42,48,49
   48  DVC=2.0
       ALT=ALT+ZD
       PSI=PSI-VT*CRV*SIGNF(TAU,PSI)
       MP=2
       GO TO 40
   49  CALL SORT
       GO TO 38
   42  VG=SQRTF(Z(9,1)**2+(EM*Z(3,1)-Z(8,1))**2)
       B=Z(9,1)/VG
       BB=(EM*Z(3,1)-Z(8,1))/VG
       DO 102 N=1,NEND
       IF (DATA(N,4,MP)) 101,101,103
  101  DATA(N,2,MP)=0.
       DATA(N,3,MP)=0.
       DATA(N,1,MP)=0.
       GO TO 102
  103  DST=VG*(DATA(N,4,MP)-DATA(NV,4,MP))
       DATA(N,2,MP)=DATA(N,2,MP)+DST*BB
       DATA(N,3,MP)=DATA(N,3,MP)-DST*B
  102  CONTINUE
       PRINT 204, KASE,EM,ALT
       PRINT 203
       PRINT 208
       PRINT 209,(PHI(N),(DATA(N,J,MP),J=1,4),N=1,NEND)
   38  IF(JOBS)311,310,310
  311  CALL EXIT
  200  FORMAT(6I10)
  201  FORMAT(F10.0,4F10.3)
  202  FORMAT(7F10.2)
  203  FORMAT(19H0SHOCK-GROUND DATA )
  204  FORMAT(18H1SONIC BOOM, CASE I5,5H,  M=F6.3,12H,  ALTITUDE=F7.0)
  205  FORMAT(18H1SONIC BOOM, CASE I5,5H,  M=F6.3,12H,  ALTITUDE=F7.0,7H,
     1  ACC=F7.3,5H, RC=F4.2,5H, VF=F6.3,5H, LF=F6.3/1H ,5H  WT=F9.1,9H,
     1 LENGTH=F6.1,6H,  FR=F5.2,5H, WL=F6.3,8H, ANGLE=F7.2,6H, TAU=F6.2,
     1 4HSEC.12H, CURVATURE=F7.3/1H0)
  206  FORMAT (1H08X8HALTITUDE7X8HHEADWIND8X8HSIDEWIND8X8HPRESSURE4X11HSO
     1UND SPEED4X11HTEMPERATURE/11X4H(FT)11X5H(FPS)11X5H(FPS)11X5H(PSF)8
     2X5H(FPS)9X7H(DEG F)/1H )
  207  FORMAT (1H F15.0,3F16.3,F13.3,F15.3)
  208  FORMAT(1H0,9X,5HANGLE,7X,13HPRESSURE JUMP, 6X,1HX,15X,1HY,10X,4HTI
     1ME/1H ,9X,5H(DEG),10X,5H(PSF),9X,4H(FT),12X,4H(FT),9X,5H(SEC)/1H )
  209  FORMAT(1H ,F14.2,F15.3,2F15.0,F13.2)
  210  FORMAT(1H0,43HHISTORY OF SHOCK STRENGTH VARIATION, ANGLE= F6.2)
  211  FORMAT(1H0,11X,1HZ,15X,1HX,15X,1HY,8X,45HPRESSURE RATIO     PRESSU
     1RE JUMP     PRESSURE/1H , 9X,4H(FT),12X,4H(FT),12X,4H(FT),31X,5H(P
     1SF),10X,5H(PSF)/1H )
  212  FORMAT(1H ,3F15.0,F19.7,F17.3,F15.3)
  213  FORMAT(1H0,38HGROUND IS CLOSER THAN 100 BODY LENGTHS)
  214  FORMAT(24H0CUTOFF ALTITUDE, ANGLE=F6.2)
  215  FORMAT(42H0CUTOFF BEFORE 100 BODY LENGTHS, ALTITUDE=F10.2,8H, ANGL
     1E=F6.2)
  216  FORMAT(56H0ACCELERATION EFFECTS BEFORE 100 BODY LENGTHS, ALTITUDE=
     1F10.2,8H, ANGLE=F6.2)
  217   FORMAT (38H0COMPUTATION DOES NOT CONVERGE, ANGLE=F6.2)
       END
```

```
      SUBROUTINE CCRR
     DIMENSION Z(9,100),S(9),W(9),X(9),Y(9),PJ(7),Q(9),AY(9),DATA(21,5,
    1 2),PHI(21)
     COMMON Z,KEND,CTH,STH,C,B,S,G,KQ,DL,H,R1,W,X,C1,Y,F,VS,VP,C2,AY,PJ
    1,BSV,BSA,PHI,DATA,PR,U,AVS,JNR,NEND,ALT,EL,Q,EZ,BSC,ELH,KASE,EM,EN
    1,N,ACC,RC,BONG,NV,NN,JOBS,WT,T,WL,VF,FL,APR,BVP,TEST,AF,HH
      COMMON CRV,PSI,TAU, PS,TS,XD,YD,ZD ,VT,MP
      VALF(X)=SQRTF(1.0+(ALF+2.0*BETA*X)**2)
      CRV=CRV*1.0E-06
      PSI=PSI/57.2957795
      IF (PSI) 3,4,3
4     PSI=ABSF(PSI)
3     TS=SIGNF(TAU,PSI)
      VT=SQRTF(((EM*Z(3,1))*COSF(PSI)-Z(8,1))**2+((EM*Z(3,1))*SINF(PSI)
    1)**2)
      ALF=-TANF(PSI)
      BETA=0.5*CRV*(1.0+ALF**2)**1.5
      XD=0.
      QUAD=0.
      DO 1 I=1,10
      IF (XD) 11,12,11
11    QUAD=(VALF(0.)+4.0*VALF(XD/2.0)+VALF(XD))*XD/6.0
12    XI=XD
      XD=XI-(QUAD-TS*VT)/VALF(XI)
      IF(ABSF((XD-XI)/XD)-0.01) 2,2,1
1     CONTINUE
      PRINT 1100,XI,XD
1100  FORMAT (1H014HERROR MESSAGE.2X53HX CORRECTION FOR CURVED FLIGHT P
    1ATH DID NOT CONVERGE./1H0)
2     ZD=(XD*BETA+ALF)*XD
      YD=-TS*Z(9,1)
      IF (ZD) 5,5,44
44    IF (PSI) 45,46,45
45    XD=-XD
      YD=-YD
      ZD=-ZD
      PSI = PSI-VT*CRV*TS
      GO TO 5
46    PSI=  TAU*VT*CRV
5     PSI=PSI*57.2957795
      RETURN
     END(1,1,0,0,0,1,1,1,0,0,0,C,0,0,0)
```

```
      SUBROUTINE SORT

      SUBROUTINE SORT
     DIMENSION Z(9,100),S(9),W(9),X(9),Y(9),PJ(7),Q(9),AY(9),DATA(21,5,
    1 2),PHI(21) ,J(21) ,SG(21,5)
     COMMON Z,KEND,CTH,STH,C,B,S,G,KQ,DL,H,R1,W,X,C1,Y,F,VS,VP,C2,AY,PJ
    1,BSV,BSA,PHI,DATA,PR,U,AVS,JNR,NEND,ALT,EL,Q,EZ,BSC,ELH,KASE,EM,EN
    1,N,ACC,RC,BONG,NV,NN,JOBS,WT,T,WL,VF,FL,APR,BVP,TEST,AF,HH
      COMMON CRV,PSI,TAU, PS,TS,XD,YD,ZD ,VT,MP
      NSUM=2*NEND
      TAVG=0.
      DO 10 N=1,NEND
      J(N)=2
      IF(DATA(N,4,2))11,11,12
11    DO 110 L=1,3
110   DATA(N,L,2)=0.
      J(N)=1
      GO TO 10
12    DATA(N,4,2)=DATA(N,4,2)-TS
      DATA(N,3,2)=DATA(N,3,2)+YD
      DATA(N,2,2)=DATA(N,2,2)+XD
10    IF (DATA(N,4,1))13,13,14
13    DO 130 L=1,3
130   DATA(N,L,1)=0.
      J(N)=1
14    IND=J(N)
      GO TO (15,16),IND
15    NSUM=NSUM-2
      GO TO 100
16    TAVG=TAVG+DATA(N,4,1)+DATA(N,4,2)
100   CONTINUE
      IF (NSUM) 17,17,18
17    K=1
      GO TO 300
18    K=2
      TAVG=TAVG/FLOATF(NSUM)
      DO 200 N=1,NEND
      IND=J(N)
      GO TO (21,22),IND
21    DO 210 L=1,3
210   SG(N,L)=0.0
      GO TO 200
22    B=(DATA(N,4,1)-TAVG)/(DATA(N,4,1)-DATA(N,4,2))
      DO 220 L=1,3
220   SG(N,L)=DATA(N,L,1)-B*(DATA(N,L,1)-DATA(N,L,2))
200   CONTINUE
300   PRINT 1100,KASE,EM
1100  FORMAT(18H1SONIC BOOM, CASE I5,5H,  M=F6.3/
     1       1H0,9X,5HANGLE,7X,13HPRESSURE JUMP, 6X,1HX,15X,1HY,10X,4HTI
     1ME/1H ,9X,5H(DEG),10X,5H(PSF),9X,4H(FT),12X,4H(FT),9X,5H(SEC)/1H0
     1 18H  RAY-GROUND DATA )
      ALTI=ALT-ZD
      PRINT 1101,ALTI,(PHI(N),(DATA(N,L,1),L=1,4),N=1,NEND)
      PRINT 1101,ALT ,(PHI(N),(DATA(N,L,2),L=1,4),N=1,NEND)
1101  FORMAT (12H0ALTITUDE = F7.0/(F15.2,F15.3,2F15.0,F13.2))
      PRINT 1102
1102  FORMAT (1H0/19H0SHOCK-GROUND DATA /1H0)
      GO TO (301,302),K
301   PRINT 1103
1103  FORMAT (1H021HNO SHOCK-GROUND DATA.)
      RETURN
302   PRINT 1104,(PHI(N),(SG(N,L),L=1,3),TAVG,N=1,NEND)
1104  FORMAT (F15.2,F15.3,2F15.0,F13.2)
      RETURN
     END(1,1,0,0,0,1,1,1,0,0,0,0,0,0,0)
```

APPENDIX IV

CLIMBING, DIVING, AND FLIGHT PATH CURVATURE EFFECTS

AIV.1 RAY ANGLE GEOMETRY

In this section we will describe an extension to the general theory which is given in Appendix I. This extension will permit inclusion of flight paths which are curved, climbing, or diving. The results, however, are restricted to aircraft motions which are in a vertical plane. The contributions which arise from lateral motions can be determined by going through geometrical arguments very similar to those given below.

To include diving and climbing effects in the general theory we first introduce a new coordinate system (x*, y*, z*).

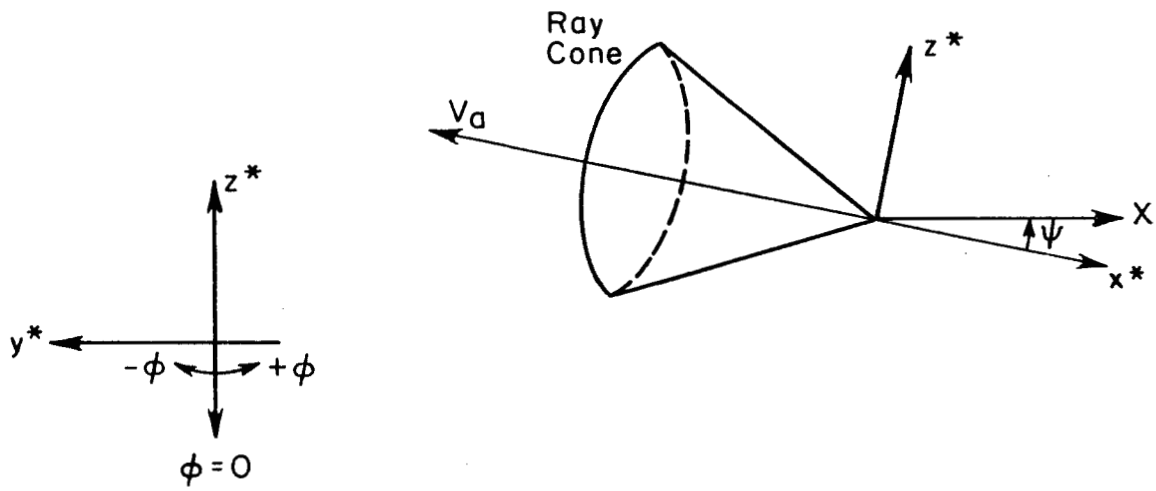

Figure A IV. 1

x* is tangent to the flight path and the velocity is in the negative x* direction, y* is perpendicular to x* and is horizontal, z* is perpendicular to y* and x* and points upward. The coordinates (x*, y*, z*) are to form a right-handed system, and the aircraft is moving in the x*, z* plane. The angle ϕ will be used to identify any ray in the initial ray cone (see Fig. A IV. 1) This angle has the same meaning as that defined in Fig. II.1, page 5 and Fig. 1, page 31. Any unit vector in the initial ray cone (which is normal to the initial shock cone) has components relative to x*, y*, z* , given in

terms of Mach angle and rotation angle ϕ:

$$\left.\begin{aligned} N_{x^*} &= -\sin\mu \\ N_{y^*} &= -\cos\mu\sin\phi \\ N_{z^*} &= -\cos\mu\cos\phi \end{aligned}\right\} \qquad \text{(A IV..1)}$$

For climbing aircraft the angle ψ, between x* and (horizontal) X is positive; for diving aircraft ψ is negative. That is, ψ is measured from the x* to the X axes, positive in the counterclockwise direction. The components of unit vector N, given in (A IV.1), relative to X, Y, Z coordinates are

$$\left.\begin{aligned} N_X &= -\sin\mu\cos\psi - \cos\mu\cos\phi\sin\psi \\ N_Y &= -\cos\mu\sin\phi \\ N_Z &= \sin\mu\sin\psi - \cos\mu\cos\phi\cos\psi \end{aligned}\right\} \qquad \text{(A IV.2)}$$

We now want to construct the "ray coordinate system" x, y, z. Recalling (see discussion below Eq. (A.11) of Appendix I) that the angle θ is determined by requiring the ray to be initially in the x, y, z plane; we let ℓ, m, n be the x, y, z direction cosines of the unit vector N.

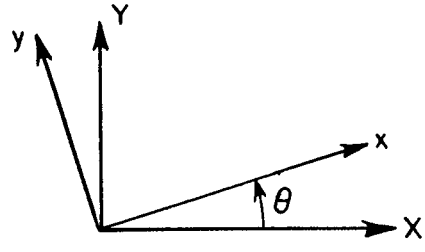

Rotating about the Z = z axis:

$$\left.\begin{aligned} \ell &= N_X\cos\theta + N_Y\sin\theta \\ m &= N_X\sin\theta + N_Y\cos\theta \\ n &= N_Z \end{aligned}\right\} \qquad \text{(A IV.3)}$$

In order to have m = 0:

$$\left.\begin{aligned} \tan\theta &= \frac{N_y}{N_x} = \frac{\cos\mu \sin\phi}{\sin\mu \cos\psi + \cos\mu \cos\phi \sin\psi} \\ \sin\theta &= \frac{N_y}{\sqrt{N_y^2 + N_x^2}}, \quad \cos\theta = \frac{N_x}{\sqrt{N_y^2 + N_x^2}} \end{aligned}\right\} \quad \text{(A IV.4)}$$

Combining the results of Eqs. (A IV.3) and (A IV.4), the initial x direction cosine of the ray is

$$\ell_h = -\cos\mu \sqrt{\left[\tan\mu \cos\psi + \cos\phi \sin\psi\right]^2 + \sin^2\phi} \qquad \text{(A IV.5)}$$

Eqs. (A IV.4) and (A IV.5) reduce to Eqs. (3.3) and (3.4) of Appendix I when the climb or dive angle ψ equals zero. Also, all the results of Appendix I can be applied using the more general definitions given in (A IV.4) and (A IV.5).

The results presented in this section make it possible to determine the ray locations and shock strengths for aircraft on straight climbing or diving flight paths. However the technique used for determining the shock-ground intersection curve (see page 15) is inapplicable to the diving-climbing aircraft problem. This is because for each instant along the flight path, the rays leaving the aircraft will have a different ground intersection curve. The main reason for this is that the aircraft altitude is continuously changing. The technique developed on page 15 assumes that each set of ray-ground intersections is the same and to know any one implies knowledge of all, therefore a shock-ground curve can be constructed although the rays that meet it have left the aircraft at different times. In the third section of this appendix we will describe a method for determining an approximate shock-ground intersection.

It is not too difficult to include aircraft flight path curvature in the analysis. This is of considerable importance for determining the ray tube area used in shock strength computations. If the flight path is concave downward, two successive rays will be directed toward each other in a manner very similar to that of an accelerating aircraft. At some point below the aircraft the rays will converge leading, locally, to a high shock overpressure. The theory for this will be derived in the next section.

AIV.2 FLIGHT PATH CURVATURE

In Section IV.2, page 25, perturbations to the ray inclination angle, ν, were found. These perturbations arise from two effects; the first, $\Delta_1 \nu$, is the initial difference in the slopes of two successive rays due to aircraft acceleration. If the aircraft were flying on a curved flight path there would be an additional contribution to the difference $\Delta_1 \nu$. We will derive this second contribution in this section.

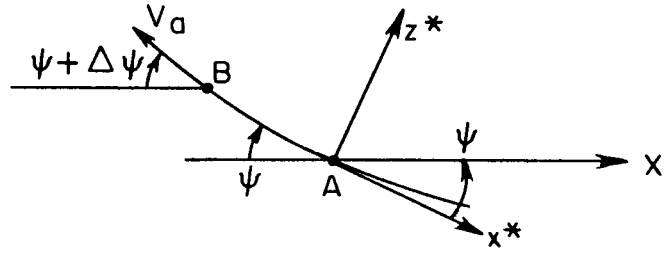

At the initial point, A, the flight path is at an angle ψ with respect to the horizontal; at point B (assumed to be an infinitesimal distance from A) the angle has changed to $\psi + \Delta\psi$. Relative to a coordinate system setup at B, the components of a unit vector, identified by the angle $\overline{\phi}$, in the ray cone has components (see Eq. (AIV.1).

$$\left.\begin{aligned} \overline{N}_x &= -\sin\mu \\ \overline{N}_y &= -\cos\mu \sin\overline{\phi} \\ \overline{N}_z &= -\cos\mu \cos\overline{\phi} \end{aligned}\right\} \qquad \text{(AIV.6)}$$

The bar notation is used to indicate variables at point B. In order to relate the components of $\overline{N}$ in (A IV.6) to the x*, y*, z* system we must rotate an amount $\Delta\psi$ about the y axis. Keeping terms of first order in $\Delta\psi$; i.e., sin $\Delta\psi$, cos $\Delta\psi$ = 1

$$\left.\begin{aligned} \overline{N}_{x^*} &= -\sin\mu - \cos\mu\cos\overline{\phi}\,\Delta\psi \\ \overline{N}_{y^*} &= -\cos\mu\sin\overline{\phi} \\ \overline{N}_{z^*} &= \sin\mu\,\Delta\psi - \cos\mu\cos\overline{\phi} \end{aligned}\right\} \qquad \text{(A IV.7)}$$

We now must identify the angle $\overline{\phi}$ with the angle ϕ used in the previous section. At point A, we passed a plane through the x* axis making an angle ϕ with the vertical (see Fig. A IV.1). At point B we passed a plane through the $\overline{x}$ axis making an angle $\overline{\phi}$ with the vertical. In order that the two rays, corresponding to ϕ at A and $\overline{\phi}$ at B, lie in the same plane, defined by ϕ, we must have

$$\frac{N_{y^*}}{N_{z^*}} = \tan\phi = \frac{\cos\mu\sin\overline{\phi}}{\cos\mu\cos\overline{\phi} - \sin\mu\,\Delta\psi} \quad . \qquad \text{(A IV.8)}$$

Letting $\overline{\phi} = \phi + \Delta\phi$ we obtain from (A IV.8)

$$\Delta\phi = -\sin\phi\tan\mu\,\Delta\psi \qquad \text{(A IV.9)}$$

We can now determine the change in initial ray direction due to changes in both aircraft Mach number and flight path slope. First we recall the identity

$$\sin\nu = -\ell$$

therefore

$$\Delta_1\nu = -\sec\nu_h\,\Delta\ell_h \, . \qquad \text{(A IV.10)}$$

By using (A IV.5) we can determine

$$\left.\begin{aligned} \Delta \ell_h &= \frac{\partial \ell_h}{\partial \mu} \frac{d\mu}{dM} \Delta M + \frac{\partial \ell_h}{\partial \psi} \Delta \psi \\ \text{where } \sin \mu &= 1/M, \quad \frac{d\mu}{dM} = -\left(M \sqrt{M^2-1}\right)^{-1}, \quad \Delta M = \frac{\Delta V_a}{a_h} \end{aligned}\right\} \text{(A IV.11)}$$

After carrying out the differentiations in (A IV.11), using (A IV.9), and substituting the result in A IV.10) we obtain, finally:

$$\Delta_1 \nu = -\sec \nu_h \left[\frac{\Delta v_a \cos^2 \nu_h}{M(M^2-1) a_h \left| \ell_h \right|} \left\{ 1 - \frac{\sin \psi}{\cos^2 \nu_h} \left(\sin \psi - \cos \phi \sqrt{M^2-1} \right) \right\} \right.$$

$$\left. - \frac{\Delta \psi \cos \phi}{M} \left\{ \cos \theta \left(\cos \psi \sqrt{M^2-1} - \sin \psi \cos \phi \right) - \sin \theta \sin \phi \right\} \right]$$

(A IV.12)

It is easily shown that for a straight and level flight, $\psi = \Delta\psi = 0$, Eq. (A IV.12) reduces to Eq. (IV.9) on page 26. Of the terms multiplying $\Delta\psi$, the one $\cos \theta \cos \psi \sqrt{M^2-1}$ is largest. Therefore the coefficient of $\Delta\psi$ is positive and a negative curvature, $\Delta\psi < 0$, has the same effect as a positive acceleration. For an accelerating, climbing (take off) flight path the effects of a positive acceleration and curvature will offset each other. Similarly for a decelerating, diving (landing) flight path the negative acceleration and curvature offset each other.

With $\Delta_1 \nu$ given in (A IV.12) the ray tube area term (see Eqs. (IV.12)

and (III.2)) is

$$A = z \sec \nu_h \left[1 - s \left\{ \frac{\dot{V}_a \left[M^2 (M^2 - 1) \right]^{-1}}{a_h^2 \, | \, \ell_h \, | \cos \theta} \left(1 - \frac{\sin \psi}{\cos^2 \nu_h} \left[\sin \psi - \cos \psi \cos \phi \sqrt{M^2 - 1} \right] \right) \right. \right.$$

$$\left. \left. - k \frac{\cos \phi}{M \cos^2 \nu_h} \left(\cos \psi \sqrt{M^2 - 1} - \sin \psi \cos \phi - \tan \theta \sin \phi \right) \right\} \right.$$

$$\left. + \frac{\sec \nu_h}{V_a \cos \theta} \int_h^z \tan \nu \left(\frac{dV_s}{dz} - \sin \nu \, \frac{du_0}{dz} \right) dz \right] \qquad \text{(A IV.13)}$$

The term k is the rate of change of flight path angle with respect to distance along the flight path

$$\text{i.e., } k = \frac{1}{V_a} \frac{d\psi}{dt}$$

This is, by definition, the flight path curvature.

The curvature can be related to aircraft motions as follows: Consider a curved flight path,

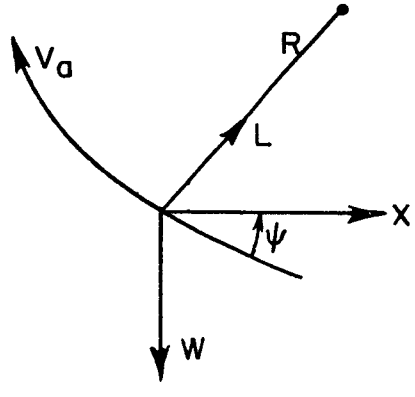

L = lift
W = weight
R = radius of curvature

Figure A IV.2

with the (simplified) force diagram as shown in Fig. AIV.3. Balancing the radial forces at the instantaneous center of curvature

$$\frac{W}{g}\ \frac{V_a^2}{R} = L - W \cos \psi$$

$$\text{therefore } k = \frac{1}{R} = \frac{(L - W \cos \psi) g}{W V_a^2}$$

When lift, L, is greater than W cos ψ the aircraft is increasing its flight path angle and the curvature is positive; when L is smaller than W cos ψ the curvature is negative.

AIV.3 SHOCK GROUND INTERSECTION

When an aircraft is either climbing or diving the shock-ground intersection curve varies with time. The problem is, therefore, basically different from the one in which the aircraft is flying horizontally. This latter problem is truly a steady state situation and the shock-ground intersection curve is invariant.

The shock-ground curve is the locus of disturbances which reach the ground simultaneously. By integrating the ray equations (III.1) we obtain the locus of disturbances which leave the aircraft at the same time. There are many ways to determine a shock curve when ray curve data are known; however the one chosen, and described below, seems to be comparatively simple and uses a minimum of computer time.

Two points on the flight path are determined which are separated, in time, by an increment τ. Then, the ray ground intersections are computed for each of these points. To be specific, assume data are determined for seven angles ϕ about the flight path; therefore the computer determines seven ray-ground X, Y coordinates, seven ray travel times, and seven pressure jumps for each of the two points on the flight path. A mean ray travel time is then found by simply averaging the fourteen computed travel times; i.e.,

$$t_{mean} = \frac{1}{14} \sum_{i=1}^{7} (t_{Ai} + t_{Bi}) \qquad \text{(AIV.14)}$$

where t_{Ai} or t_{Bi} is the ray travel time from point A or B on the flight path corresponding to angle ϕ_i. Then, using this mean time, we determine by linear interpolation (or extrapolation) the corresponding X, Y coordinates and the pressure jump Δp as follows:

$$X_{i\ mean} = X_{Ai} + \frac{t_{Ai} - t_{mean}}{t_{Ai} - t_{Bi}} (X_{Bi} - X_{Ai}) \qquad \text{(A IV.15)}$$

with the identical formula being used with Y or Δp substituted for X.

The resulting coordinates are, approximately, the ground intersection points of disturbances (shock) arriving at the ground simultaneously. The pressure jumps are the pressure jumps across this shock.

It is recognized that the above computation gives some hypothetical "mean" shock and its strength. This is simply intended as an aid in visualizing the ground-shock pattern. The computer will print out the ray-ground data for both flight path points as well as the derived shock data, and the operator can interpret all the data as he so desires.

A IV.4 PROGRAM DETAILS

Program Inputs

The last three entries on the "aircraft data cards" (see page 6) are the flight path curvature (1/ft), the climb or dive angle (deg), and the time increment τ (sec) between the two flight path points. Since the curvature is usually a very small number it is to be read in as (curvature) x 10^6. A positive curvature indicates the flight path angle is increasing, and a negative curvature indicates a decreasing flight path angle. A climbing aircraft will have a positive flight path angle, and a diving aircraft a negative angle. The time increment between flight path points has been left as an input for the convenience of the operator. It has been found that a five-second interval has led to satisfactory results.

Program Calculations

If both the curvature and the climb (or dive) angle are zero the SBCP will operate as described in the main body of this report. If either one or both are nonzero two additional subroutines are used. These are named CORR and SORT. These will be described below.

SUBROUTINE CORR - In this subroutine the second point on the flight path is determined, assumeing that the first point is at the origin. Since motion in the vertical X, Z plane the flight path can be approximately described as

$$\left.\begin{aligned} & z = \alpha x + \beta x^2 \\ \text{with} \quad & \alpha = -\tan \psi, \ \beta = 1/2\, k\, (1+\alpha^2)^{3/2} \\ & \psi = \text{flight path angle (see Fig. A IV.1)} \\ & k = \text{flight path curvature} \end{aligned}\right\} \qquad \text{(A IV.16)}$$

If the aircraft flight path velocity (see Fig. A IV.3) relative to a fixed coordinate system were denoted V_T, we can write

$$V_T = \sqrt{\dot{x}^2 + \dot{z}^2} = -\frac{dx}{dt}\sqrt{1 + (\alpha + 2\beta x)^2} \qquad \text{(A IV.17)}$$

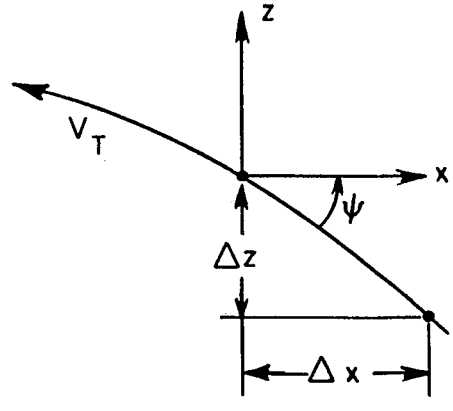

Figure A IV.3

Integrating (A IV.17) over the time increment τ, assuming V_T is constant

$$\tau V_T + \int_0^{\Delta x} \sqrt{1 + (\alpha + 2\beta x)^2}\, dx = 0 \qquad \text{(A IV.18)}$$

solution of (AIV.18) for Δx gives the x coordinate of the second point on the flight path, this is accomplished in subroutine CORR by a Newton-Raphson iteration. Equation (AIV.16) is then used to determine Δz. In subroutine ALTA all atmospheric data above the flight altitude are discarded. This means that whenever two points on the flight path are used the higher one must be computed first. Subroutine CORR takes care of all situations for diving, climbing or level flight.

SUBROUTINE SORT - In this subroutine the computed ray-ground data, for the two flight pathpoints, are referred to a common origin and time scale. The linear interpolation described in Eqs. (AIV.14 and 15) is then carried out, and finally all the data is printed.

APPENDIX V

EXPERIMENTAL RESULTS

In this section the results of several computations with the SBCP will be presented. For all the cases described the same aircraft model was used. Different flight and atmospheric conditions were investigated. The necessary aircraft parameters were:

weight	= 100,000 lbs.	volume factor	= .64
length	= 100 ft.	lift factor	= .6
max dia.	= 12 ft.		

The basic atmosphere, unless otherwise indicated, was taken from ARDC 1959 Model Atmosphere.

Figure A V.1

This figure indicates the ground-shock intersection curve for an aircraft flying above a jet stream. Superimposed on the ARDC atmosphere the jet stream starts at 50,000 ft., builds up linearly to 200 ft/sec at 35,000 ft and then falls to zero again at 20,000 ft.

Five cases were tested. These were aircraft velocity 0° (parallel), 45°, 90° (cross jet), 135°, 180° (anti-parallel) to the jet stream direction. For all cases, effects on pressure jump across the shock were negligible by time the shock reached the ground. While propagating through the jet stream the shock strength ($\Delta p/p$) tends to increase when in a region where the headwind (tailwind) is increasing (decreasing); conversely shock strength tends to decrease when the headwind (tailwind) is decreasing (increasing). For all cases the variation within the jet stream was at most 10% from the uniform atmosphere case.

The three cases shown in Fig. AV.1 are uniform (no jet stream) atmosphere solid line; 45° jet stream, dash dot line; 90° (cross wind) dashed line. The groups of symbols correspond, reading from left to right, to ϕ angles 45°, 30°, 15°, 0°, −15°, −30° −45°. To facilitate identification the alternate angle symbols (45°, 15°, −15°, −45°) are filled in. It is interesting to note that the −45° ray for the 45° direction

jet stream gets cut off and never reaches ground. The -45° ray, cross-wind case nearly gets cut off; it does get to the ground but considerably further out than the uniform atmosphere case.

Figure AV.2

For this case a perturbation on the ARDC temperature profile was introduced. A sample perturbation is shown in the left figure. Four cases are shown in the right figure.

1. standard atmosphere
2. temperature inversion and return to standard, centered at 10,000 ft.
3. temperature inversion and return to standard, centered at 5,000 ft.
4. temperature inversion between 5,000 ft. and ground.

In case (4) the temperature fell from standard at 5,000 ft. to about 25° F at the ground. For all cases the pressure jump decreases (increases) when the shock propagates into an increasing (decreasing)temperature region.

It should be noted that for a standard atmosphere the shock strength, Δp, remains nearly constant for almost all of its travel near the ground. See, for example, case (1). The reason for this is that although the pressure ratio $\Delta p/p$ is decreasing with distance in accordance with Whitham's theory, the ambient pressure, p, is increasing as the ground is approached. These two effects counterbalance each other and Δp remains nearly unchanged.

A further comment can be made. Almost all atmospheric perturbations which occur above about 15,000 ft. altitude are "forgotten" by time the shock reaches the ground. That is, it is only those phenomena occurring near the ground which will affect the shock strength at the ground.

Figure AV.3

Acceleration effects at different Mach numbers are investigated here. The Mach number has a pronounced effect on the location of the high pressure, due to focusing, region. Due to limitations of the ray tube approach the magnitude of the pressure jump at its peak value may

not be too accurate, however the location is correct. For all cases shown the shock directly below the aircraft is considered.

The pressure drops off considerably, after the high pressure peak. Also the pressure jump at the ground, for the M = 1.2 case for example is close to that which would occur for a nonaccelerating aircraft at the same initial flight condition. For the M = 1.1 case the shock is cut off before it reaches the ground, due to the increasing temperature as the ground is approached. For the M = 1.3 case the shock gets to the ground before the pressure peak is reached.

Note that the buildup to the pressure peak takes place over an extended region, approximately 10,000 ft for the M = 1.2 case. Whereas the actual, unusually high pressure region is quite localized.

Figure AV.4

For this case we considered the effect of a temperature inversion and acceleration induced pressure peaks near the ground. Conditions were setup so that for a standard atmosphere the pressure peak occurs at about 1000 ft altitude.

A temperature profile was introduced which was standard to 5,000 ft and then fell to 24°F at the ground. The effect of the inversion was to cause the pressure peak to occur sooner, i.e., at a higher altitude. The location of the pressure peak had, within the limitations of the present theory, very little effect on its magnitude.

Figure AV.5

This case was essentially the same as that shown in Figure AV.4 except that the aircraft altitude was 50,000 ft. For a standard atmosphere the shock meets the ground before the pressure peak occurs. However, when a temperature inversion, near the ground, is inserted the pressure peak occurs sooner; i.e., above the ground. The boom at the ground for this latter case, is actually less than that for the standard atmosphere plus acceleration case. If the ground altitude were about 2,000 ft. the boom in the presence of a temperature inversion could be much greater than the standard atmosphere case.

Figure AV.6

In this figure the effects of flight path curvature and aircraft acceleration are shown. A hypothetical (nonrealistic) situation was constructed to indicate the general shock behavior. The atmosphere was assumed to be constant with a sound speed equal to about 1000 ft/sec. This same atmosphere was used for problem on p. 42. In addition, an aircraft dive angle of 15 degrees was assumed.

The output for case 1 of Fig. AV.6 is given on the page following this figure. This output is typical of one for problems which include diving or climbing aircraft on curved flight paths as described in Appendix IV. Also, this output can be compared with the one on page 42 to see the difference in the ground effects between a horizontal flight and a diving flight. For the case on page 42 the pressure jump at the ground is lower although the aircraft Mach number was higher. This is due to the fact that for a diving aircraft the shock travel distance is less.

In case 1 of Figure AV.6 no acceleration or curvature effects were introduced. For case 2 an acceleration of 36.4 ft/sec^2 was used. For case 3 a flight path curvature of -14.5×10^{-6} $ft.^{-1}$ was chosen to cause a pressure peak at approximately the same altitude as for case 2. Case 4 shows the additive nature of these two effects, half the acceleration and half the curvature were used. For case 5 a positive curvature was introduced, this just cancelled the acceleration effects.

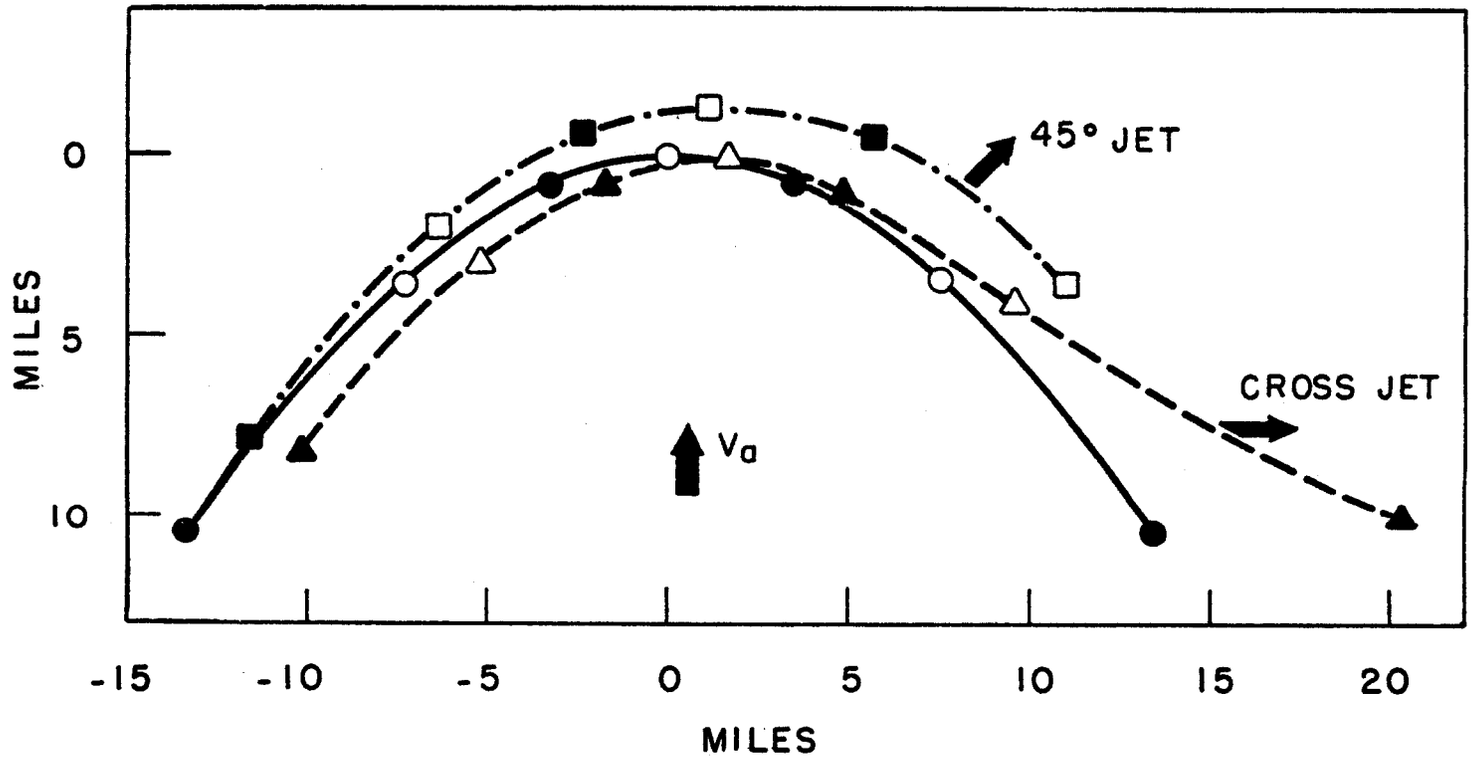

Figure AV.1. Shock-ground curves, M = 2, alt. = 60,000 ft, jet stream at 35,000 ± 15,000 ft.

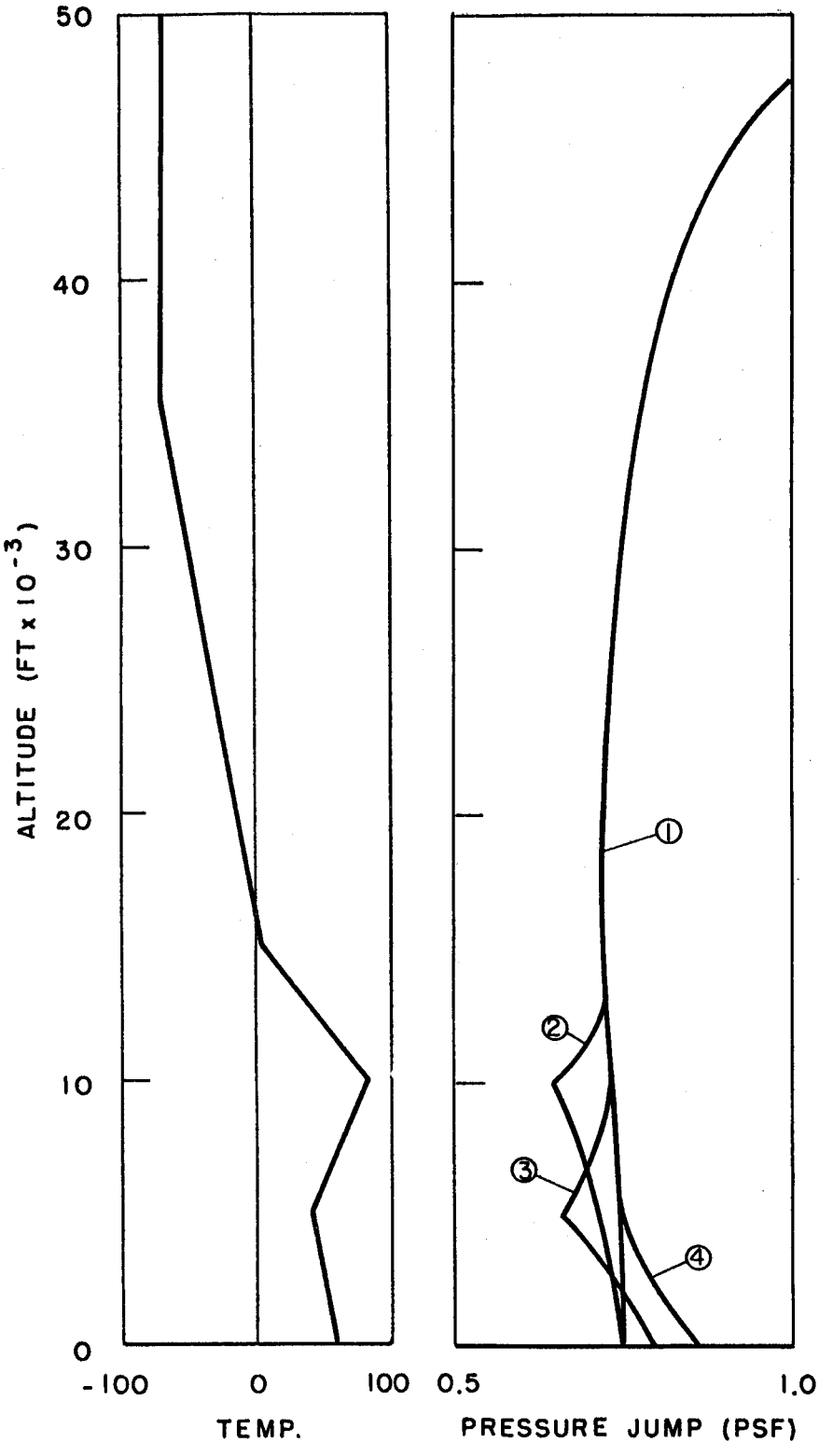

Figure AV.2. Temperature inversion, M = 2, alt. = 60,000 ft.

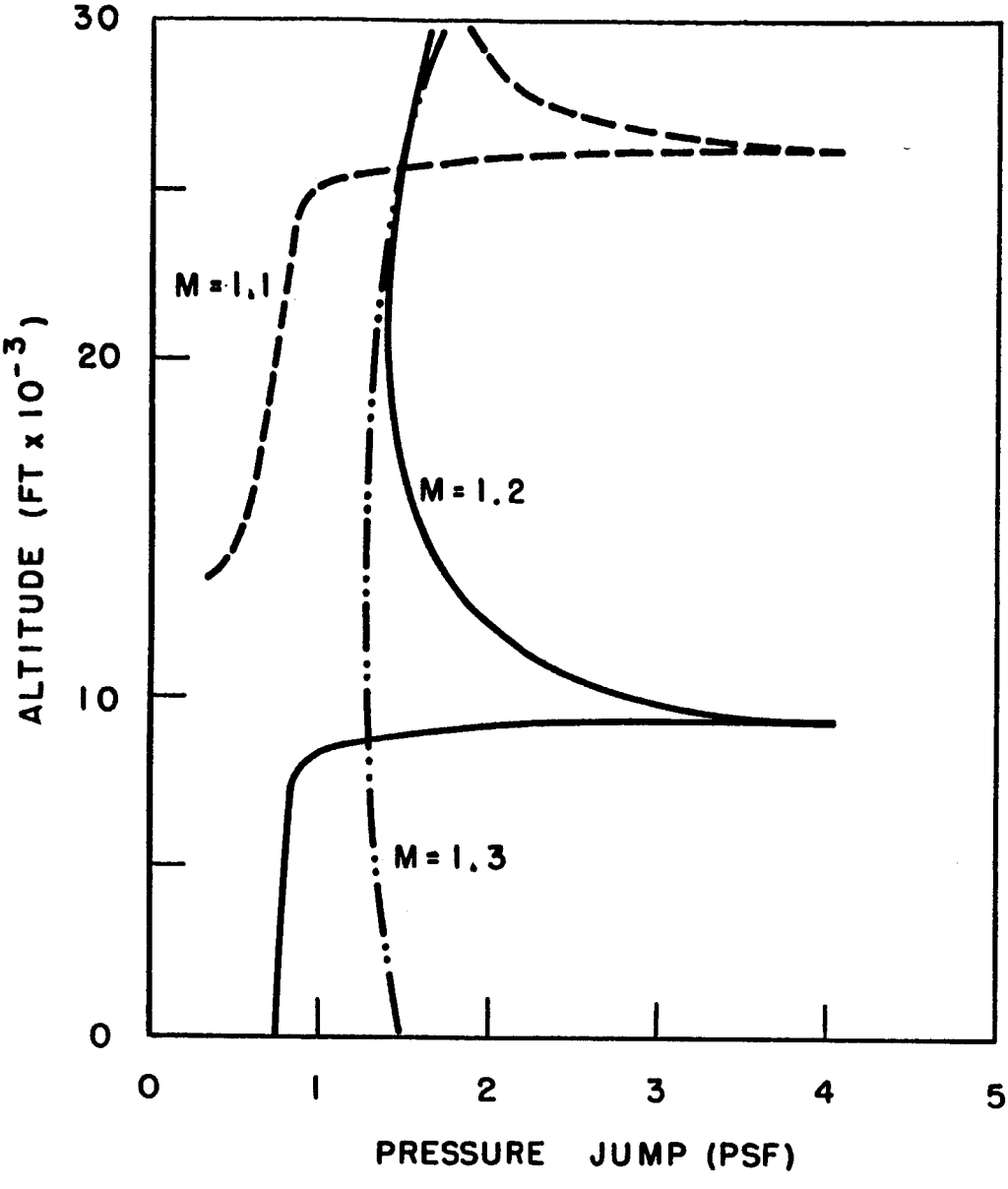

Figure AV.3. Acc'l. aircraft, st'd atmos., alt. = 40,000 ft.

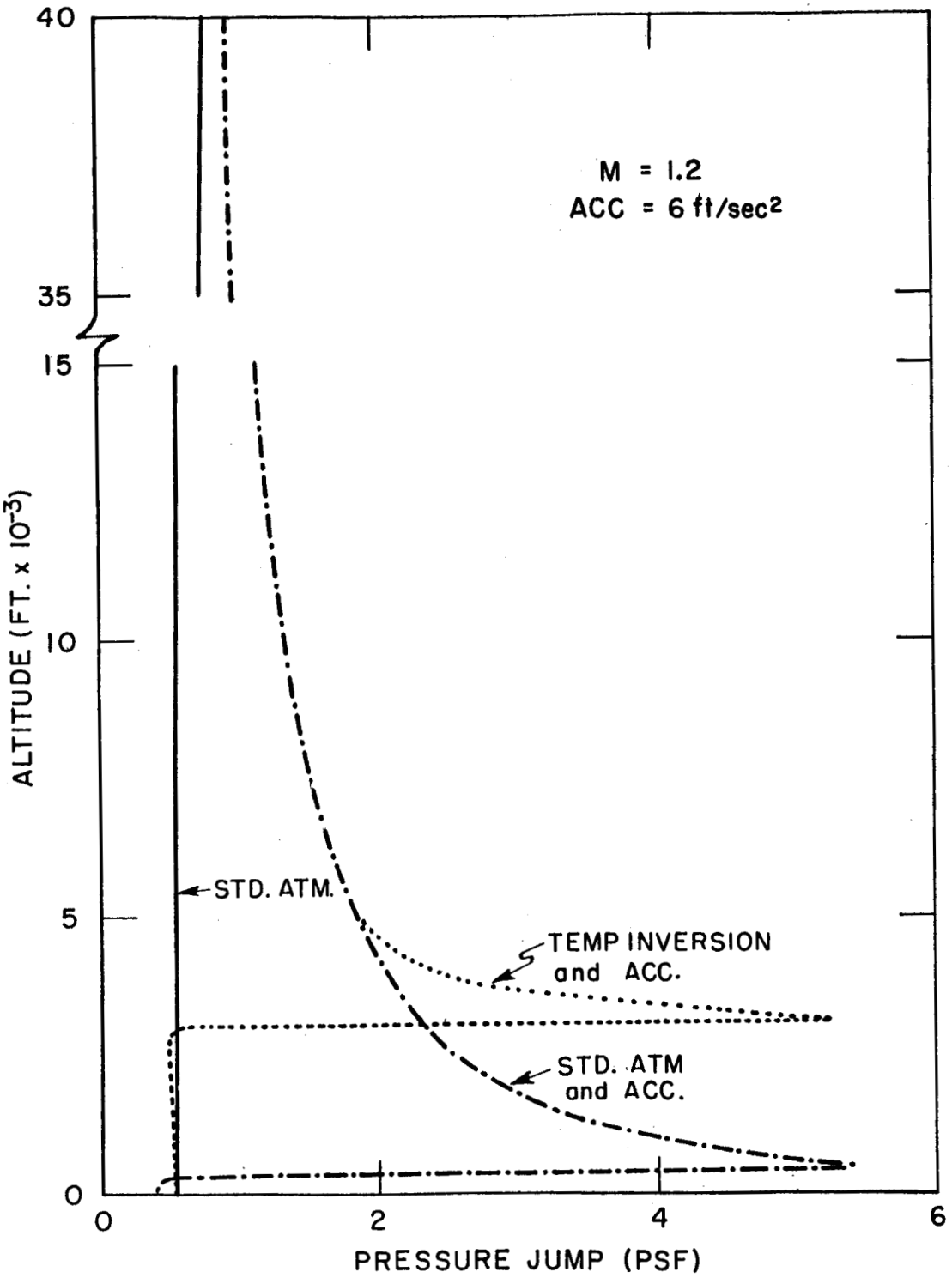

Figure AV.4. Aircraft accel. and temp. inversion, alt. = 56,000 ft.

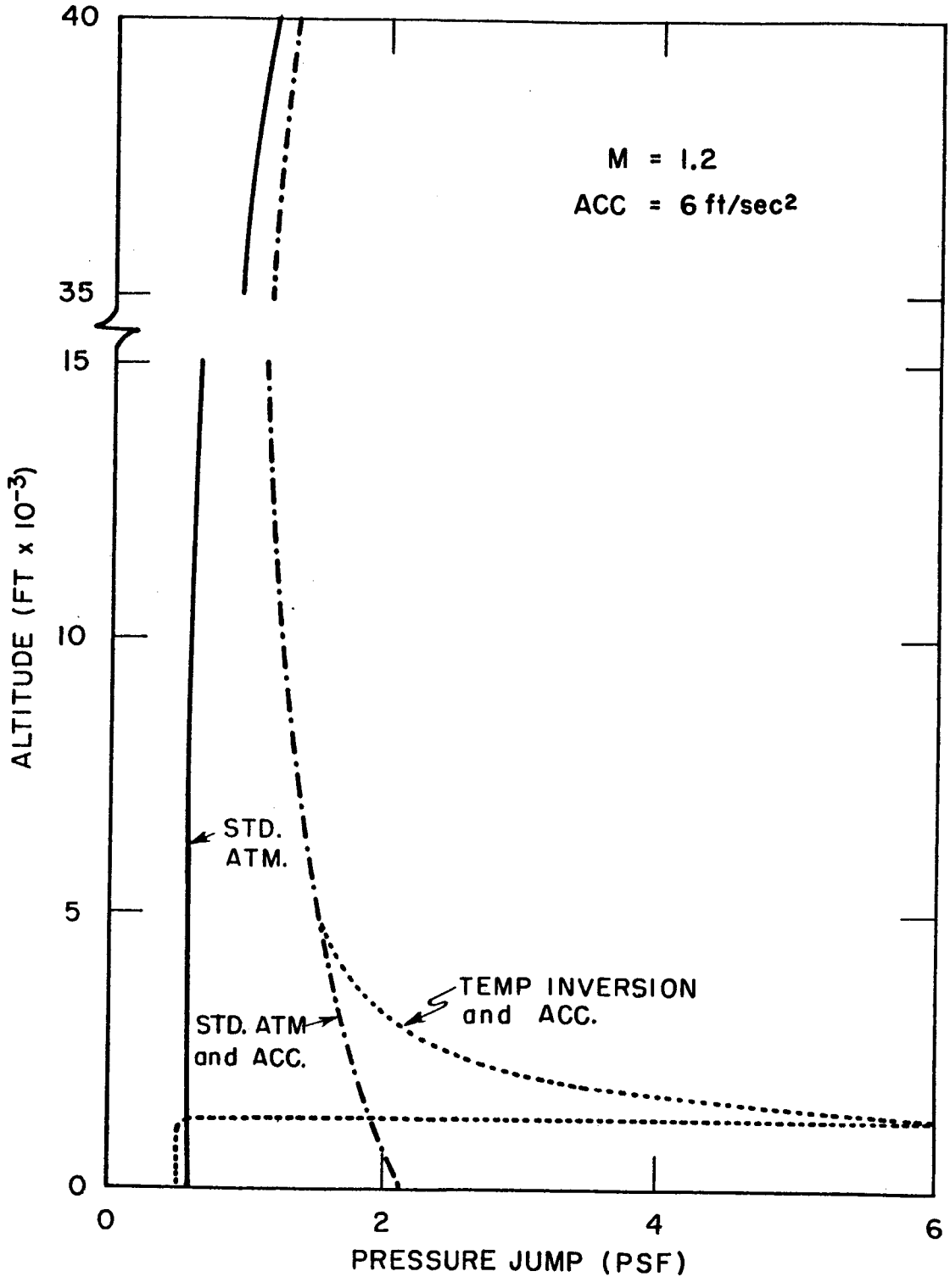

Figure AV.5. Aircraft accel. and temp. inversion, alt. = 50,000 ft.

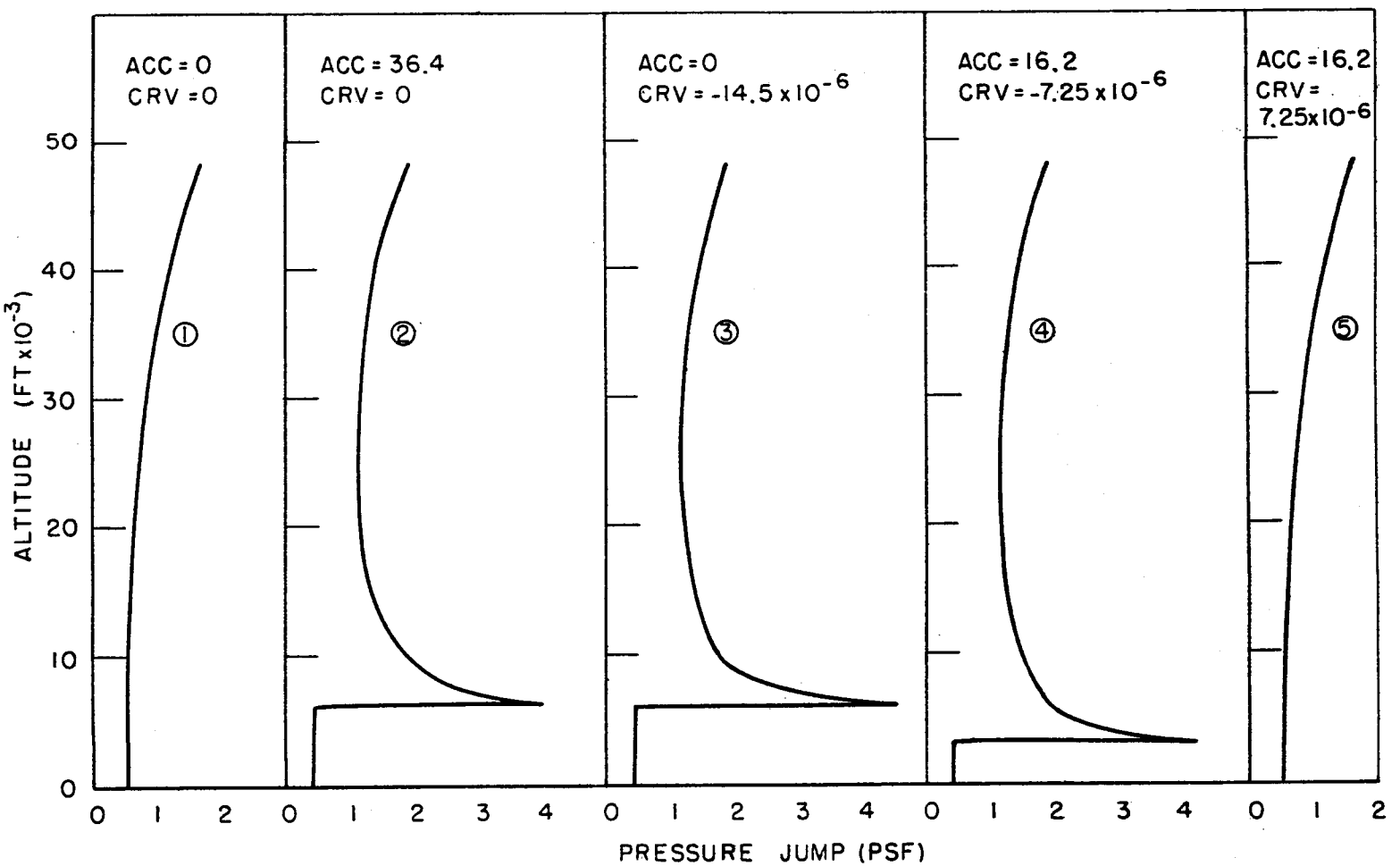

Figure AV.6. Aircraft acceleration and flight path curvature, dive angle = 15°, M = 1.5, alt. = 60,000 ft.

SONIC BOOM, CASE 0, M= 1.500, ALTITUDE= 60000., ACC= 0. , RC=1.80, VF= 0.640, LF= 0.
WT= 100000.0, LENGTH= 100.0, FR= 8.00, WL=50.000, PSI= -15.00, TAU= 5.00SEC., CURVATURE= 0.

ALTITUDE (FT)	HEADWIND (FPS)	SIDEWIND (FPS)	PRESSURE (PSF)	SOUND SPEED (FPS)	TEMPERATURE (DEG F)
60000.	-0.	-0.	657.600	998.446	-44.400
8000.	-0.	-0.	657.600	998.446	-44.400
0.	-0.	-0.	657.600	998.446	-44.400

HISTORY OF SHOCK STRENGTH VARIATION, ANGLE= 0.

Z (FT)	X (FT)	Y (FT)	PRESSURE RATIO	PRESSURE JUMP (PSF)	PRESSURE (PSF)
48000.	-6065.	-0.	0.0025819	1.698	657.600
46000.	-7077.	-0.	0.0023288	1.531	657.600
44000.	-8089.	-0.	0.0021082	1.386	657.600
42000.	-9101.	-0.	0.0019286	1.268	657.600
40000.	-10113.	-0.	0.0017807	1.171	657.600
38000.	-11125.	-0.	0.0016569	1.090	657.600
36000.	-12137.	-0.	0.0015590	1.025	657.600
34000.	-13148.	-0.	0.0014614	0.961	657.600
32000.	-14160.	-0.	0.0013870	0.912	657.600
30000.	-15171.	-0.	0.0013175	0.866	657.600
28000.	-16183.	-0.	0.0012548	0.825	657.600
26000.	-17194.	-0.	0.0011985	0.788	657.600
24000.	-18206.	-0.	0.0011476	0.755	657.600
22000.	-19217.	-0.	0.0011016	0.724	657.600
20000.	-20228.	-0.	0.0010596	0.697	657.600
18000.	-21240.	-0.	0.0010212	0.672	657.600
16000.	-22251.	-0.	0.0009859	0.648	657.600
14000.	-23262.	-0.	0.0009533	0.627	657.600
12000.	-24273.	-0.	0.0009231	0.607	657.600
10000.	-25285.	-0.	0.0008950	0.589	657.600
8000.	-26296.	-0.	0.0008689	0.571	657.600
6000.	-27307.	-0.	0.0008486	0.558	657.600
4000.	-28318.	-0.	0.0008226	0.541	657.600
2000.	-29329.	-0.	0.0008043	0.529	657.600
0.	-30341.	-0.	0.0007810	0.514	657.600

SONIC BOOM, CASE 0, M= 1.500

ANGLE (DEG)	PRESSURE JUMP (PSF)	X (FT)	Y (FT)	TIME (SEC)
RAY-GROUND DATA				
ALTITUDE = 60000.				
-30.00	0.850	-35971.	28111.	75.47
0.	0.924	-30341.	-0.	67.31
15.00	0.904	-31654.	-13344.	69.21
30.00	0.850	-35971.	-28111.	75.47
ALTITUDE = 58062.				
-30.00	0.873	-42043.	27203.	78.04
0.	0.947	-36594.	-0.	70.13
15.00	0.928	-37865.	-12913.	71.98
30.00	0.873	-42043.	-27203.	78.04
SHOCK-GROUND DATA				
-30.00	0.829	-30595.	23915.	73.21
0.	0.971	-43396.	0.	73.21
15.00	0.939	-40629.	-12721.	73.21
30.00	0.829	-30595.	-23915.	73.21